Numerical modelling of spatio-temporal variability of growth of *Mytilus edulis* (L.) and influence of its cultivation on ecosystem functioning

Tomasz Dabrowski*[1], Kieran Lyons[1], Marcel Curé[2], Alan Berry[1], Glenn Nolan[1]

[1]Marine Institute, Rinville, Oranmore, Co. Galway, Ireland
[2]The Numerics Warehouse Ltd., Tyrone, Kilcolgan, Co. Galway, Ireland

Corresponding author: Tomasz Dabrowski
Marine Institute, Rinville, Oranmore, Co. Galway, Ireland
E-mail: tomasz.dabrowski@marine.ie
Phone: +353 91 387367
Fax: +353 91 387201

Abstract

One of the key needs of the aquaculture industry is the implementation of effective management methods to ensure the sustainability, economic viability and minimization of negative impacts on both human and ecosystem well-being. The authors developed a Fortran 90 implementation of the dynamic energy budget (DEB) model for *Mytilus edulis*. The model has been further developed to include physiological interactions with the ecosystem and coupled to a biogeochemical nutrient-phytoplankton-zooplankton-detritus (NPZD) model. Phytoplankton and detritus uptakes, oxygen utilization, CO_2 production, NH_4 excretion, egestion of faeces, and assimilation of food are modelled. A novel approach was derived that accounts for the allocation of C and N in mussel flesh and shell organic fraction. The DEB-NPZD model has been subsequently coupled to a high resolution three dimensional numerical coastal ocean model of the south-west coast of Ireland, where approximately 80% of national rope mussel is produced annually. Simulations have been carried out for the time period July 2010 – June 2011, for which the field data on mussel biometrics and ambient seawater properties were collated. The model accurately reproduced the spatio-temporal variability in blue mussel growth. It is also shown that the ecosystem dynamics is affected by the presence of aquaculture farms. The modelling system presented allows for the assessment of the impacts of aquaculture activities on water quality, quantification of the production and ecological carrying capacities and improvement of our understanding of the ecosystem functioning with particular emphasis on interactions between various trophic levels.

Keywords: DEB theory; *Mytilus edulis*; biogeochemical model; phytoplankton dynamics; nutrient dynamics; numerical modeling.

1. Introduction

Aquaculture is still the fastest growing food-producing sector in the world, although the figures show that the overall rate of growth, while still substantial, is not of the order seen in the 1980s and 1990s. In the period 1970–2008, the production of food fish from aquaculture increased at an average annual rate of 8.3 percent. The Food and Agriculture Organisation of the United Nations reported the annual production of 52.5 million tonnes for 2008 with an estimated value of US$98.4 billion (FAO, 2010). In Europe, the growth of 14.2% in the years 2000-2008 was reported; however, in the European Union a decline of 8.4% was recorded in the same time period (FAO, 2010), partly due to market factors, and also due to the introduction of stringent regulations. In Ireland, the total shellfish production doubled in years 1990-2007, and rope mussel production recorded a growth of c.230% in tonnage in the same time period (Browne et al., 2008).

One of the key needs of the aquaculture sector is the implementation of effective management methods to ensure the sustainability, economic viability and minimization of negative impacts on both human health and the environment. Both human and ecosystem well-being and their harmonization have been implicitly promoted in recent environmental legislation, such as the European Union's Water Framework Directive (EC, 2000) and Marine Strategy Framework Directive (EC, 2008). The directives aim at achieving good ecological status of all surface inland and coastal waters in the coming decade. This presents major challenges to various regulatory bodies responsible for sustainable management of water resources. Sustainable management of water resources is also at the core of sustainable management of aquaculture.

The analysis and management of coastal embayments and shellfish aquaculture is nowadays supported by different computer tools, varying in complexity from highly aggregated, low data requirements (e.g. ASSETS; Bricker et al., 2003), through tools addressing production and ecological sustainability at a finer spatial scale (e.g. Ferreira et al., 2007) to more detailed and complex research models. Examples of the latter include box models for analysis of mussel carrying capacity (Filgueira and Grant, 2009), ecosystem models for food depletion (Grant et al., 2008), and 2D and 3D biogeochemical models (Brigolin et al., 2009; Cugier et al., 2010; Duarte et al., 2003; Duarte et al., 2007; Ferreira et al., 2008; Grangeré et al., 2009; Guyondet et al., 2010; Maar et al., 2009; Marinov et al., 2007; Nunes et al., 2011; Ren et al., 2010).

In recent years, considerable research has been carried out on the application of the Dynamic Energy Budget (DEB) theory (Kooijman, 2010) to simulate growth and bio-energetics of various bivalve species, and the interest in DEB models is increasing. DEB models have been successfully applied to several shellfish species including *Mytilus edulis* (e.g. Handå et al., 2011; Filgueira et al., 2011; Maar et al., 2009; Rosland et al., 2009, 2011; Saraiva et al., 2011a;

Thomas et al., 2011; van der Veer et al., 2006), *Crassostrea gigas* (e.g. Alunno-Bruscia et al., 2011; Barillé et al., 2011; Bernard et al., 2011; Bourlès et al., 2009; Emmery et al., 2011), and other species. Several authors have dynamically coupled DEB models with biogeochemical models to provide feedbacks from aquaculture farms to phytoplankton and nutrient dynamics. Grangeré et al. (2010) and Grangeré et al. (2009) accounted for food uptake, biodeposition and excretion of the Pacific oyster, with ammonia excretion rates arbitrarily specified as a fraction of ingested nitrogen. In both studies, food uptake was calculated from the predicted filtration rates and converted from energy to mass units using appropriate conversion factors. Maar et al. (2009) studied local effects of blue mussels around an off-shore wind farm and reported significant changes in the ecosystem dynamics, which were confirmed by field data, when the model included ingestion of microplankton and copepods, excretion of ammonia and egestion of faecal pellets. Details of the formulations applied were, however, not provided. Ren et al. (2010) and Guyondet et al. (2010) coupled the DEB model for mussels with the ecosystem models within the framework of numerical models and included the uptake of food, excretion and biodeposition. In the former study, the mussels feed only on the phytoplankton, whereas in the latter the mussel food is made of phytoplankton, detritus and zooplankton using the preference ratios. Other efforts to model the impacts of shellfish on phytoplankton and nutrient dynamics include that of Cugier et al. (2010), who developed an ecological model for Mont Saint Michel Bay, France, and accounted for filtration rates of several filter-feeder species by including additional sinks and sources for food proxies and detrital matter, respectively. Grant et al. (2008) and Brigolin et al. (2009) coupled the mussel models based on the Scope for Growth concept (e.g. Newell et al., 1998) with the biogeochemical models. In the former study the interactions were limited to food uptake and biodeposition, whereas in the latter the authors specified C, N and P fluxes associated with food uptake, excretion and faeces and pseudo-faeces production for the species of *Mytilus galloprovincialis*. Finally, Saraiva et al. (2011b) used the concept of the Synthesizing Units, which is part of the DEB theory, to describe the main feeding processes in bivalves; however, this approach is yet to be tested in the application to a real case study.

The aim of this study is to present a new method for modelling the interactions between *Mytilus edulis* and the ecosystem developed by the authors and discuss the results obtained from its application to Bantry Bay in the south-west of Ireland. The authors developed the Dynamic Energy Budget (DEB) model (Kooijman, 2010) to include these interactions and linked it with the Nutrient-Phytoplankton-Zooplankton-Detritus (NPZD) model (Fennel et al., 2006), whilst allowing for the exchange of fluxes between the two models. Modelled shellfish physiological processes include: food ingestion, respiration, excretion and faeces production. A novel approach is derived that accounts for the allocation of C and N in mussel's flesh and shell organic fraction.

The proposed DEB-NPZD model has been coupled to a high resolution 3D numerical model of a coastal region of the south-west of Ireland featuring an intensive bivalve aquaculture actitivity. The modelling system aims to provide an understanding and a tool for the quantification of the environmental impacts of aquaculture farming. The methodology given here should assist in the estimation of the production and ecological carrying capacity on the regional and local scale and thus supporting the determination of ecological status of coastal waters.

2. Model description

2.1 The Mussel Ecophysiological Model

The authors developed the implementation of the DEB algorithm (Kooijman, 2010) for *Mytilus edulis* in Fortran 90. The advantage of the DEB model lies in its versatility and generality, with its application to other species only requiring a new set of parameters and only minor modifications to the code. Implementations vary from annelids to mammals and a database with codes and parameters is maintained at the VU University Amsterdam at http://www.bio.vu.nl/thb/. The reader is referred to van der Veer et al. (2006), van der Meer (2006) and Rosland et al. (2009) for detailed formulations of the model for shellfish; here only the main features of the model are provided.

The DEB theory describes the uptake and utilisation of the energy by an organism throughout its lifecycle. In the implementation presented here, the filter-feeder ingests the energy at a rate proportional to its surface area and dependent on food availability through a Holling type II functional response and temperature through the Van't Hoff-Arrhenius equation. Part of the ingested energy is assimilated and enters the reserve pool. A fixed fraction, κ, of this energy is spent on somatic maintenance and growth (with a priority for maintenance), and the rest goes to maturity, reproduction and maturity maintenance (so-called κ-rule). The energy allocated to reproduction is converted to eggs and the reproductive buffer is emptied at spawning. Spawning occurs when the threshold values for the gonado-somatic index and temperature are reached. It can also be forced at spawning dates known from the observations. In the case of prolonged starvation when the energy reserves are too low to support maintenance costs, the energy can be withdrawn from the reproductive buffer through lysis of the gonadic tissue leading to shrinking of the total flesh weight. Basic set of equations for this implementation of the DEB theory is presented in Table 1.

The model has three state variables, namely the structural body volume, V, the energy reserves, E, and the reproductive energy, E_r. These are summarized in Figure 1 along with the biogeochemical model state variables. Two additional parameters are calculated from these state

variables: shell length, *L*, from the relationship $L = V^{1/3} / \delta$, where δ is the shape coefficient, and dry flesh weight, *DW*, from the following equation:

$$DW = \psi_{DW\_WW} \cdot V \cdot \rho + \frac{(E + E_r) \cdot \psi_{DW\_WW}}{\mu_E \cdot \psi_{AFDW\_WW}} \quad (1)$$

where ρ is the structural volume density (g cm^{-3}), μ_E is the energy content of the reserves in ash free dry weight, AFDW, (J g^{-1}), Ψ_{AFDW_WW} is the conversion factor from wet weight, WW, to AFDW, and Ψ_{DW_WW} is the conversion factor from wet weight to dry weight.

The parameterization from van der Veer et al. (2006) was implemented except for the following parameters: somatic maintenance costs, fraction of utilized energy spent on maintenance and growth, shape coefficient and half saturation constant for food, which were established for the considered study area; details are given in section 4.1.

2.2 The Biogeochemical Model

The biogeochemical module is based on the nutrient-phytoplankton-zooplankton-detritus model (NPZD) developed by Fennel et al. (2006). The code was originally developed to examine the budget of nitrogen on a continental shelf and to compare different major pathways of transport: riverine flux, cross-shelf break transport, the removal of biologically available nitrogen by denitrification in the sediments, and therefore fluxes between the model's compartments are calculated in the units of nitrogen. This also implies that the emphasis of the model architecture is not to provide any kind of differentiation between phytoplankton groups as primary producers, or the zooplankton, which are lumped together as one group of grazers.

The phytoplankton growth in the NPZD model is a function of light (P-I relationship), temperature (Eppley relationship) and nitrate and ammonium concentrations (Michaelis-Menten relationship). Grazing is represented by a Holling type S shaped curve to limit grazing at high phytoplankton concentrations. The mortality of phytoplankton is simply proportional to the concentration, and for zooplankton it is proportional to the concentration squared. The deceased plankton (as well as unassimilated food) goes into the small detritus pool and these aggregate into large detritus at a fixed rate. Both fractions have their own sinking velocities. Within the benthos, the model instantaneously remineralises, nitrifies (consumption of oxygen and ammonium) and de-nitrifies a portion of the particulate matter arriving at the sediment sea interface. The model is extended to include the oxygen and carbon sub-modules. The model's state variables are presented in Figure 1 and the full set of equations for the basic implementation of this model are described in Fasham et al. (1990) and Fennel et al. (2006).

2.3 Coupling Between Ecophysiological and Biogeochemical Model

The authors have coupled the models described in sections 2.1 and 2.2 to include the following processes: food uptake and assimilation of nitrogen and carbon in bivalve, egestion of faeces, NH_4 excretion, oxygen utilization and CO_2 production. A schematic diagram of the coupled model is presented in Figure 1 and details of the governing equations are provided below. As the NPZD model used in this study is based on nitrogen, most of the equations in this section are written for nitrogen. Similar formulations can be derived to describe carbon cycling.

Respiration rate is proportional to the energy utilisation rate ($\dot{p}_C$, J d^{-1}), (Pouvreau et al., 2006), and the oxygen utilisation rate (O_C , mgO_2 d^{-1}) can be written as:

$$O_C = \frac{\dot{p}_C}{\eta} \tag{2}$$

where η is a constant for converting oxygen to energy equivalents and equals 14.3 J mg^{-1} O_2 (Gnaiger and Forstner, 1983).

The energy ingestion rate in the DEB model is proportional to the surface area of the structural body volume and the dimensionless response function, f, which scales the ingestion rate in relation to food concentration, *X*, according to a Holling type II function:

$$f = \frac{X}{X + X_K} \tag{3}$$

where X_K is the half saturation coefficient. Chlorophyll_a (*Chla*) was used as a food proxy in this study in order to calculate *f*. The mussel food is made of phytoplankton and small detritus in the presented model and their time rates of change due to an uptake by an individual mussel are given by following equations:

$$\frac{dP_N}{dt} = -\frac{P_N}{P_N \cdot P_{CN} + \mu_M \cdot SD_C} \cdot C_{ing} \tag{4}$$

$$\frac{dSD_N}{dt} = -\frac{\mu_M \cdot SD_C}{P_N \cdot P_{CN} + \mu_M \cdot SD_C} \cdot \frac{C_{ing}}{S_{CN}} \tag{5}$$

where P_N is phytoplankton N (mmol N m^{-3}), *t* is time (d), P_{CN} is phytoplankton C:N ratio and is equal to 6.625, μ_M is the food selection factor set at 0.5 following Guyondet et al. (2010), SD_C is small detritus C (mmol C m^{-3}), S_{CN} is small detritus C:N predicted by the model, and C_{ing} is the carbon ingestion rate by an individual mussel. C_{ing} is calculated from:

$$C_{ing} = \frac{\dot{p}_X}{P_{EC} \cdot c_f} \tag{6}$$

where $\dot{p}_X$ is the energy ingestion rate predicted by the DEB model (J d^{-1}), P_{EC} is the energetic value of the phytoplankton C (11.4 cal mg^{-1} C after Platt and Irwin (1973)), and c_f is the conversion factor from calories to joules (4.189 J cal^{-1}). Small detritus carbon, SD_C, and *Chl* state variables are also updated accordingly using S_{CN} and carbon:chlorophyll, *CChl*, ratios, respectively. It is assumed that the energetic value of SD_C is the same as of phytoplankton C. Since *CChl* changes due to the effects of photoacclimation, it is modelled according to the formulations given in Geider et al. (1997) and Geider et al. (1998).

In the DEB model, a fixed portion of the energy acquired from the environment is assimilated and enters the energy reserves. For the species of *Mytilus edulis* the assimilation efficiency, *AE*, equals 0.75 (van der Veer et al., 2006). The remaining energy is egested in faeces and enters the large detritus pool (LD_N and LD_C) of the model:

$$\frac{dLD_N}{dt} = (1-AE)\cdot\frac{C_{ing}}{S_{CN}}\cdot\left(\frac{P_N\cdot S_{CN}+\mu_M\cdot SD_C}{P_N\cdot P_{CN}+\mu_M\cdot SD_C}\right) \qquad (7)$$

and similarly for LD_C.

The present model accounts for the allocation of C and N in the mussel flesh and shell organic fraction, and allocates the remaining portion of C and N to respiration and excretion, respectively. In order to calculate the rates of allocation of C and N in the mussel tissue we use the following conversions: 1g AFDW = 23 kJ and 1 g AFDW = 0.4 g C (van der Veer et al., 2006). Following the study on resource allocation in *Mytilus edulis* in suspended cultures in Ireland carried out by Rodhouse et al. (1984) we assume the ratio of C:N, M_{CN}, equal 4.82 in the biomass. This value is close to the ratio of 4.87 assumed by Brigolin et al. (2009) for *Mytilus galloprovincialis*. The rate of allocation of N in a mussel flesh is given as:

$$\frac{dM_{fN}}{dt} = \frac{AFDW_C\cdot(\dot{E}_V+\dot{E}+\dot{E}_r)}{\mu_E\cdot M_{CN}\cdot m_a} \qquad (8)$$

where M_{fN} represents the amount of N allocated in mussel flesh (mmol N), $AFDW_C$ is the fraction of AFDW that is carbon, $\dot{E}_V$ is the energy flux to somatic tissue (J d^{-1}), $\dot{E}$ the energy flux to reserves (J d^{-1}), $\dot{E}_r$ the energy flux to the reproductive buffer (J d^{-1}), and m_a is an atomic mass of N. Similar equation can be derived for the amount of C allocated in mussel flesh, M_{fC}, by removing M_{CN} from equation (8) and using the atomic mass of carbon.

M_{fC} and M_{fN} constitute 92% and 88% of the total allocation of C and N, in the biomass, respectively (Rodhouse et al., 1984). An additional 8% of C, M_{shC}, and 12% of N, M_{shN}, are allocated in the shell organic fraction (Rodhouse et al., 1984). Finally, the ingested food that has not been egested in faeces or allocated in flesh or shell is respired as CO_2 in the case of C, C_r,

and excreted as NH_4 in the case of N, N_{ex}. The rate of ammonium excretion is thus given by:

$$\frac{dNH_4}{dt} = AE \cdot \frac{C_{ing}}{S_{CN}} \cdot \left(\frac{P_N \cdot S_{CN} + \mu_M \cdot SD_C}{P_N \cdot P_{CN} + \mu_M \cdot SD_C}\right) - \frac{(1 + f_E \cdot 0.136) \cdot AFDW_C \cdot (\dot{E}_V + \dot{E} + \dot{E}_r)}{\mu_E \cdot M_{CN} \cdot m_a} \quad (9)$$

where f_E equals 1 when the total energy flux is into the mussel to account for allocation in shell and 0 when the total energy flux is out of the mussel (lysis).

A conceptual diagram of the coupled eco-physiological and biogeochemical model is presented in Figure 1 and the parameterization is summarized in Table 2.

3. Model application

3.1 Study site

The model was applied to Bantry Bay located in the southwest of Ireland, which is one of the most important national regions for shellfish culture; see Figure 2. Approximately 80% of national rope mussel (*Mytilus edulis*) is produced here annually (Browne et al., 2008). The industry is located in the bays of Bantry, Dunmanus and Long Island formed by glaciations forming drowned river valleys also known as rias. In Bantry Bay the annual rope mussel production varied between 1952 and 4648 tonnes in recent years.

Bantry Bay exhibits limited estuarine behaviour becoming thermally stratified in the summer months (Raine et al., 1990) with weak tidal currents, typically below 5 cm s^{-1}. Circulation is thus primarily wind driven; this is also due to the fact that the bay is axially aligned to the predominant wind direction from the southwest (Edwards et al., 1996). When the bay is thermally stratified, variations in wind direction cause two layer oscillatory flows which generally result in the import of water from the near coastal continental shelf containing phytoplankton (Edwards et al. 1996), and in general water flushing is in an anticlockwise direction, which has implications for nutrient availability for shellfish culture. Substantial mixing due to this wind driven exchange then prevents any one phytoplankton species dominating the bay (Raine et al., 1993).

Toxic algal blooms is the major problem facing the existing mussel industry in Bantry Bay, and routine testing is undertaken by the Marine Institute. Closures frequently occur for weeks or longer in extreme circumstances, for example for 10 months over the 1993-94 season (Garforth and FitzGerald, 1996).Competition for space is another problem, as production is heavily concentrated in some areas, such as Inner Bantry Bay to the east of the Whiddy Island (see Figure 2) resulting in placing long lines in more exposed areas.

Freshwater inputs to Bantry Bay are small and highly variable due to the mountainous character of the surrounding region. Five main rivers are Adrigole, Glengarriff, Coomhola, Owvane and Mealagh.
Figure 2 presents the location of Bantry Bay and distribution of rope mussel farms within it.

3.2 Numerical model

The 3D model used in this study is based on the Regional Ocean Modelling System (ROMS) which is a free-surface, hydrostatic, primitive equation ocean model described in Shchepetkin and McWilliams (2005). ROMS uses orthogonal curvilinear coordinates on an Arakawa-C grid in the horizontal while utilizing a terrain-following (sigma) coordinate in the vertical.
The model domain aligned with the main bay's axis and depicted in Figure 2 consists of 557 x 419 grid cells relating to a horizontal spacing of 200 – 250m and 20 vertical levels. The model is nested in a regional North East Atlantic model run operationally at the Marine Institute and is a refinement of the latter by a factor of five. Time series of water levels, 2D and 3D momentum, temperature and salinity are provided every 10 minutes, and all biogeochemical model state variables are provided every 3 hours at the open boundaries. The model was initialized in February 2010 from the parent model output interpolated onto a child grid. Surface forcing is taken from the half-degree Global Forecasting System (GFS) that is available at three-hourly intervals and the model interpolates data onto its current time step. Heat fluxes are calculated from the bulk formulae and freshwater fluxes are obtained from the prescribed rainfall rates and the evaporation rates calculated by the model. Surface stress is calculated using the COARE algorithm (Fairall et al., 1996). Bottom stress is applied using the logarithmic "law of the wall" with a roughness coefficient of 0.005m. Freshwater discharges from five rivers shown in Figure 2 are included in the model. The model bathymetry utilizes data from a number of sources (e.g. Irish National Seabed Survey multibeam dataset) to produce the best possible bathymetry for the area.
The parent model domain (NE_Atlantic) covers a significant portion of the North-West European continental shelf at a variable horizontal resolution between 1.2 and 2.5 km and with 40 sigma levels (Figure 2). It is nested within the high resolution (1/12°) Mercator Ocean PSY2V4R2 operational model of the North Atlantic whereby daily values for potential, temperature, sea surface height and velocity are linearly interpolated from the parent model onto the NE_Atlantic model grid at the boundaries. Tide forcing is prescribed at the model boundaries by applying elevations and barotropic velocities for ten major tide constituents, which are taken from the TPXO7.2 global inverse barotropic tide model (Egbert and Erofeeva, 2002).

The simulation presented in this paper covers the time period of 1 year from July 2010 to June 2011 for which the field data on mussel biometrics and environmental conditions was acquired. Details are given in section 3.3.

3.3 Field data

Sampling commenced in July 2010 and was performed every month until June 2011. Mussel samples were acquired from two locations, namely Snave (from 1m (SN01) and 5m (SN05) depths) and Gearhies (from 1m (GH01) and 5m (GH05) depths); see Figure 2. The former is a sheltered site in Inner Bantry Bay, where density of farms is high, whereas the latter is at an exposed location on the southern shore of the bay. Sampling was carried out at two depths: 1m and 5m and approximately 30 individuals were acquired. Shell lengths were measured along with total wet weight, dry flesh weight and wet and dry shell weights. *DW* was obtained by dissecting the mussels and drying at 60ºC for 72h. Environmental conditions were also recorded at each visit to the sites; water temperature, salinity, *pH* and *DO* were measured using a YSI 556 probe. Water samples were also acquired for the determination of chlorophyll a, NO_3, NH_4, total particulate matter (TPM), particulate organic matter (POM), particulate organic carbon (POC) and particulate organic nitrogen (PON) in the laboratory.

Additional instruments were also deployed and included Acoustic Doppler Current Profilers (ADCP), SBE-37 MicroCATs and a weather station on the Whiddy Island. Opportunistic acquisition of CTD profiles, chlorophyll a and nutrient samples was also carried out. This data was used for more in-depth validation of the operational hydrodynamic and biogeochemical model and will be presented in a separate paper.

4. Results

4.1 Calibration of the DEB model

Four DEB parameters were estimated based on the acquired datasets; these are δ, X_K, somatic maintenance costs, $\dot{p}_M$ and κ.

The shape coefficient was estimated from pooled data on *L* and *DW* from all sites. Dry weights were converted to *WW* using the conversion factor Ψ_{DW_WW} of 0.2. *WW* (g) was then converted to *V* (cm^3) assuming ρ = 1g cm^{-3}. Since in addition to the somatic tissue, *DW* also includes the energy reserves and reproductive mass, the shape parameter was tuned in order to get 5% of the observed *DW* below the fitted curve, as the curve for structural tissue should lie below the observed masses. This approach was adopted after Rosland et al. (2009). We obtained δ = 0.257, and Figure 3 shows *L* plotted against *DW*. The value of δ obtained in this study is well within the

range of 0.231 – 0.333 reported in the literature (Rosland et al., 2009 and van der Meer, 2006, respectively).

Three other DEB model parameters were tuned to the values that minimize the deviation between the observed and modelled *L* and *DW*. These parameters are X_K, κ and somatic maintenance costs, $\dot{p}_M$ (J cm^{-3} d^{-1}). Furthermore, we used TPM, POM, POC, PON, chlorophyll a and their combinations as food proxies and obtained the best fit when using chlorophyll a. This may indicate that the predominant source of food for mussels farmed in the bay is phytoplankton. We obtained X_K of 0.57 mg chla m^{-3}, κ of 0.72 and $\dot{p}_M$ of 32.3 J cm^{-3} d^{-1}; these are summarized in Table 2 along with a set of parameters related to the DEB-NPZD models interactions proposed in this study.

4.2 Validation of the hydrodynamic model

Selected results from the validation of the hydrodynamic component of the presented modelling system is provided in this section to inform on the overall predictive capability of the model as regards the underlying coastal ocean dynamics, which obviously impacts on the model's capability to represent the biological processes. As stated in section 3.3, full validation of the operational bio-physical modelling system will be presented in a separate publication.

Figure 4 summarizes the model performance as regards the prediction of tides, currents and water temperatures at various locations in Bantry Bay also shown on the figure. The tidal signal has been decomposed to individual constituents and compared against the tide gauge located in Castletownbere. A bar chart comparing the predicted and recorded amplituides of six main tidal constitutents is presented in Figure 4, and, as can be seen, high accuracy has been achieved in the model. Very good agreement was obtained for all tidal constituents, and the nested (child) model performs slightly better than the NE Atlantic (parent) model due to improved resolution and thus more accurate representation of local coastal features. Water temperatures have also been measured at two stations inside Bantry Bay by SBE-37 MicroCATs. As can be seen, the predicted and modelled temperatures are broadly similar, however, some transient events are not properly resolved by the model. In particular the model tends to overestimate most of the local minima in surface temperatures at both stations Also, the bottom temperatures appear to be slightly overestimated pointing to the possibility of excessive heating and/or mixing in the model. Nevertheless, the model represents the overall pattern, including the stratification and the time of its breakdown, well. The ADCPs were deployed at 4 locations in Bantry Bay for the period of 5 weeks in September – early October 2010. In Figure 4(d) we present an example of the time series comparison betwen the recorded and modelled current speeds (U-component) at

the North Whiddy station at mid-depth. A histogram of the depth-integrated current speeds for all stations is also presented in Figure 4. Overall, the model performance is very good, except for the Pipers station (see Figure 4(g)), where the model overestimates current speeds. This station is located in a very narrow sound to the west of the Bear Island, where modelled currents are found to be very tightly constrained in the NNE – SSW direction, with the maximum currents in the SSW direction. This is due to the grid geometry, which is not quite aligned with the channel axis and due to the grid resolution. This is the most likely reason for the worse model performance at this location when compared to other locations.

4.3 Simulation of mussel growth in the framework of the numerical model

From discussions with local growers in Bantry Bay, the majority of the licenced farms were seeded with socked dropper lines during the month of June 2010. Typical length of the socked mussels was approximately 3 cm, though this can vary between farms. From our sampling data in mid-July 2010, the average mussel length was 3.33 cm at three sites. The average length at the fourth site, GH05, was 3.57 cm. All mussel lines in Bantry Bay were harvested after approximately 1 year, when the mussels reached a commercial length of approximately 5-6 cm. The estimated harvest of mussels from Bantry Bay in 2011 was 3019 tonnes. Based on our sampling data at the four sites the average mussel weight was 7.8 g at the time of harvest, which allowed the total number of individuals to be calculated. The numerical model was initialised by distributing the individuals across the farms, in the corresponding numerical model cells, in proportion to farm sizes. An initial mussel length of 3.33 cm was specified at all farms (except GH05) commensurate with our sampled data.

The DEB model state variables were initialized as follows: bivalve length was converted to bivalve volume using equation given in Section 2.1 and the shape coefficient obtained in this study. The energy reserve was then set to 80% of the energy resulting from the maximum equilibrium energy density, E_m, for the calculated volume (E_m = 2190 J cm^{-3} after van der Veer et al. (2006)). The reproductive energy was subsequently set at the level resulting from equation (1). The simulation was then restarted and continued until end of June 2011. The interactions between an individual animal and the ecosystem described by equations (2-9) are then scaled up by multiplying the predicted rates by number of individuals in a given computational cell.

Since several physiological rates in the DEB model depend on temperature, including the food ingestion rates, it is important that the sea temperature variability is properly represented by the hydrodynamic model at the locations of our mussel sampling sites. Figure 5 presents the time series of modelled and measured water temperatures at Snave and Gearhies stations. As can be

seen in Figure 5, the model captures the annual variability in water temperatures very well. Water warms up to c. 19ºC in August and cools down to c. 7ºC in winter, dropping occasionally below 5 degrees at Snave (Figure 5(a)), as this site is more sheltered and in generally shallower waters and thus more prone to atmospheric temperature fluctuations. Temperature differences of up to approximately 2ºC between the 1m and 5m depths were observed and modelled at both sites; this seems to develop and break down quickly according to the model.

The time series of predicted *L* and *DW* are presented in Figure 6. The model reflects the annual pattern of growth well and the predictions are mostly within one standard deviation from mean, and more importantly after one year the predicted shell lengths are very close to those observed (in Bantry Bay, mussels are typically harvested c.1 year after socking them on the longlines). Little or no growth in winter across all sites is captured by the model. It is worth noting that despite the differences in the hydrographic characteristics of the two sites, data indicates the growth rate at these locations is fairly similar and averages at 0.507(0.460) at SN01, 0.453(0.456) at SN05, 0.458(0.441) at GH01 and 0.439(0.423) at GH05 mm week^{-1}, where the first figure is the observed growth rate and the figure in brackets is modelled. Although the differences are small, they are still captured by the model, which properly reflects the maximum rate at SN01 and the minimum at GH05.

As regards *DW*, it increases from c.0.2g to between c.1.2g at SN05 to c.1.6g at GH01, and the reduction in *DW* over the winter months is apparent in the data. This reduction is associated with both starvation and spawning, which is known to occur in Bantry Bay in late December or January. We imposed a spawning event in the model on the 15th of January and the energy stored in the reproductive energy compartment is reduced by 90% in 1 day. Shortly before and also after spawning *DW* still decreases since the growth is limited by low temperatures and the lack of food and mussels utilize their own energy for somatic maintenance; this is reflected in both data and the model. From March on, there is a marked increase in the *DW* across all sites and this observation is reflected well by the model, although at GH01, the model prediction for the last dataset from June 2011 is below one standard deviation, and for SN01 it is at its lower end.

Although the final *L* at the analyzed sites are similar, the model predicts more variability in spatial distribution of growth across the farms, as presented in Figure 7(a). As can be seen, the final *L* varies from 5.3 cm around the Chapel Island to the east of the Whiddy Island to 5.8 cm in Bearhaven to the north of the Bear Island and at the entrance to Adrigole Harbour. The variability of growth along the length of the dropper lines is also shown in Figure 7(b) as the difference in the predicted *L* between the bottommost and topmost ends of the dropper lines.

A sensitivity study was carried out on the standalone DEB-NPZD model in order to indicate the predictive power of the model and how the growth rates and physiological rates depend on the

model parameterization. Since the most commonly used parameter in the DEB model calibration in local implementations is X_K, four simulations were carried out for idealized conditions using the values of 0.57, 1.0, 1.5 and 2.0 for X_K. An initial L of 5 cm was assumed and the DEB model state variables were initialized as described previously. The concentration of chlorophyll a and water temperature were held constant at 1.0 mg m^{-3} and 16ºC, respectively, and the simulation was carried out for the time period of 90 days. The predicted L, C_{ing}, O_C and N_{ex} are presented in Figure 8. As can be seen, there is a substantial difference in the growth rates depending on the choice of X_K and the predicted L after 90 days varies from 5.2 to 5.8 cm for X_K of 2.0 and 0.57, respectively. Since the energy ingestion rate is a function of X_K, therefore, the carbon ingestion rates are modified accordingly. As can be seen in Figure 8, the initial C_{ing} in the model with X_K of 0.57 is two times greater when compared to the case of X_K of 2.0, and the difference is widening further as the mussels grow. The response of the model in terms of O_c and N_{ex} is somewhat less intuitive. In the case of the former, only for $X_K = 0.57$ the oxygen consumption rate increases with time indicating an increasing energy utilization rate. As regards the remaining X_K values, O_c decreases over the simulation period and the higher the X_K the lower the O_c for tested environmental conditions. In the case of the latter, its rate increases along with the growth of the mussel, and although initially N_{ex} is higher for higher X_K, its rate of increase with time is greater for lower X_K, and at the end of the simulation the greater the length, the greater the ammonia excretion rate. It can also be concluded from the analysis of Figure 8 that the rate of change in N_{ex} corresponds to the rate of change in L.

4.4 Impacts on nutrient and phytoplankton dynamics

4.4.1 Local impacts

Time series of selected model-predicted biological state variables are compared against field observations in Figure 9. Two phytoplankton blooms typically occur in NE Atlantic waters, in spring and autumn. As can be seen in Figure 9(a,b), the model captures both events both qualitatively and quantitatively. Elevated chlorophyll a levels were observed at both sites in September 2010 when compared to the months of July and August before dropping to below 0.5 mg m^{-3} and not recovering until March 2011, when an intensive bloom occurred in response to an increase in T and light. The timing of the spring bloom in the model is correct and the model predicts correct levels of chlorophyll a at all stations in March. Field data indicates low levels on the day of sampling in April and higher levels again in the following months. The modelled *Chla* also decreases in April, although the predicted concentrations are higher than measured. In general, predicted concentrations for Snave are higher than Gearhies. Measured levels at Snave show higher concentrations than at Gearhies in summer and autumn of 2010 and approximately

the same during the spring bloom of 2011. Combined with higher water temperatures at Snave when compared to Gearhies during the productive seasons (see Figure 5) this results in better growth conditions at the former site as confirmed by the average shell length observed at the end of the sampling campaign (see Figure 6).

The depletion of the phytoplankton biomass due to feeding by mussels is also apparent with larger reductions in chlorophyll a concentrations predicted for Snave stations. This also applies to POC and PON concentrations; see Figure 9(c-f). In relative terms, the highest impacts on food concentration at all monitored stations are predicted to occur in late autumn (November 2010) and at the onset of the spring bloom. It should be noted that our model underpredicts both POC and PON concentrations during the winter months and returns reasonably good predictions at other times of the year. Possible reasons are discussed in section 5. Winter NO_3 concentrations are also underpredicted at Gearhies, whereas for the remainder of the year and at Snave the model predictions agree well with the observations (see Figure 9(g,h)). The latter site is located closer to the rivers and some of the wastewater outfalls, both being the source of N and included in the model and it is reflected in more variable and higher NO_3 concentrations, predominantly in winter. Again, NO_3 enrichment caused by the excretion of NH_4 by bivalves and its further mineralization to NO_3 is more pronounced at Snave due to the higher density of farms and slower water exchange rates.

The impacts of incorporating mussel cultures on the model skill have been quantified on the Taylor diagram (Taylor, 2001) presented in Figure 10. Due to low frequency of field sampling a time window of one week, that is the day of observation ±3 days was allowed to reduce the effects of timing errors on calculated statistics. This approach is similar to the window correlation matching method presented in Piman et al. (2007) and consists of finding the observed and modelled values within the specified window so that the value of the correlation coefficient, R, is maximized. As can be seen the coupled DEB-NPZD model returns improved predictions of *Chla* at the sampling stations when compared to the scenario without mussels. The improvement is in terms of all computed statistics, R, root mean square difference, *RMSD*, and normalized standard deviation, σ. As regards POC and PON, the scenario with mussels results in turn in slightly worse performance of the model; however the correlation coefficient was already poor in the scenario without mussels, particularly for PON. The impact of mussels on the capability of the model to accurately predict NO_3 concentrations is minimal and in both cases R is above 0.9. Standard deviation is somewhat lower than that in the measured data mainly due to underprediction of NO_3 at Gearhies in winter.

4.4.2 Inner Bantry Bay and Bay Scale

Local and bay scale impacts of mussel farming on the predicted concentrations of some of the DEB-NPZD model state variables are presented in Figure 11, which shows the percentage change in predicted chlorophyll a, zooplankton, dissolved inorganic nitrogen and detritus averaged for each computational cell over the simulation period.

A general decrease in chlorophyll_a concentration is predicted by the model, mainly in Inner Bantry Bay to the east of the Whiddy Island and in Glengarriff Bay, where the concentration of mussel farms is the highest. Locally, chlorophyll_a is depleted by as much as 50%, including the area around Snave station and further south around small islands to the east of the Whiddy Island; both areas are characterized by high density of mussel farms and are also likely to receive poor flushing from the sea; see Figure 11(a). There is a slight enhancement in chlorophyll_a levels in the outer section of the bay in the areas to the south and south-west of the Bear Island. This is due to the excretion of NH_4 by the filter feeders, which adds to the DIN pool and is also a preferential nutrient for the phytoplankton. Part of this extra DIN (when compared to the run without mussels) is mixed with the incoming seawater and transported out of the bay, and therefore at a certain distance from the aquaculture farms an increase in the phytoplankton biomass, expressed here as chlorophyll_a, is predicted. This observation is also confirmed in Figure 11(b), which shows an increase in the zooplankton biomass by up to 2% in the outer section of the bay in response to higher availability of its food source. However, towards the head of the bay, reduction of the zooplankton biomass by up to 10% is predicted as a result of the competition for the same food with bivalves.

A similar spatial pattern is predicted for the detritus, being the sum of SD_N and LD_N model state variables, as shown in Figure 11(d). Reduction of up to 30% in detrital matter concentration is predicted in the inner bay as small detritus constitutes another food source for mussels in our model although the preference is shifted towards the phytoplankton as the food selection factor, μ_M, in Eq.(4) is set to 0.5. This is despite the fact that 25% of ingested small detritus and phytoplankton is rejected and egested as faeces adding to the large detritus pool ($AE = 0.75$). In the outer section of the bay, in turn, the predicted detritus concentration is up to 3% higher due to the increased productivity.

The enhancement in DIN concentration is predicted throughout the bay with the highest concentration in the inner bay and is generally in the region of 25% in the areas to the east of the Whiddy Island. In general, the enhancement in DIN concentration exhibits a positive correlation with chlorophyll_a depletion (see Figure 11(a,c)) and is linked to high concentration of farms and poor water exchange.

5 Discussion

The coupled DEB-NPZD model embedded within a 3D numerical ocean model and introduced in this paper is capable of reproducing the growth of the *M. edulis* species expressed both in terms of shell length, *L*, and dry weight, *DW*, in Bantry Bay located in the south-west of Ireland. It captures the differences in growth between the examined sites that are hydrographically different and being a 3D application it also reproduces the variability in growth throughout the water column for longline cultures as confirmed in Figures 6 and 7(b). Only at site SN05 does the model overestimate the *DW* and *L* during the winter months. However, the model performs well during the productive season, which is of more importance for better representation of feedbacks to the ecosystem and shellfish growth potential and thus for the suitability of the model as a tool for sustainable management of the aquaculture industry and coastal environments. Spatial distribution of growth in response to varying environmental conditions and the density of farms is also reflected by the model; this is important for carrying capacity studies. Being a 3D modelling system, benthic and wild populations can also be easily added to the bottommost layer. Another advantage of the presented model is the ease of its adaptation to model other filter feeder species by adopting relevant parameterization published in the literature (e.g. van der Veer et al., 2006) and available at http://www.bio.vu.nl/thb/.

Another feature that differentiates our model from the previous approaches to dynamic modelling of bivalves-ecosystem interactions (e.g. Brigolin et al., 2009; Cugier et al., 2010; Grangeré et al., 2009; Grangeré et al., 2010; Grant et al., 2008; Guyondet et al., 2010 and Ren et al., 2010); is accounting for the allocation of N and C in mussels and the way the ammonium excretion is formulated, which is important in modelling the carrying capacity of the systems, as NH_4 is the preferential nutrient for phytoplankton and will have an impact on the primary productivity also affecting the overall biogeochemical cycle. The capacity of mussel farming to alter the structure of the pelagic ecosystem has been demonstrated in Figure 11. An important observation is that enrichment in DIN caused by excretion is insufficient to mitigate the effects of the phytoplankton depletion caused by the uptake by mussels despite them acting also as an accelerator of the remineralisation rates of the detritus. Locally, the predicted chlorophyll a concentrations drop by 50% when averaged annually.

Experimental data shows that nitrogen excretion rates are related to the oxygen utilisation rates for the species of *Mytilus edulis* (Bayne and Scullard, 1977), and other bivalve species (Hawkins et al., 2002). Brigolin et al. (2009) used the ON ratio in atomic equivalents provided by Hawkins et al. (2002) for the species of *Chlamys farreri* to model the ammonia excretion rates by *Mytilus galloprovincialis*. Also, following Prins et al. (1995) who estimated that approximately 30% of primary production consumed by the blue mussel was converted into biomass, Grangeré et al.

(2009) assumed the same figure for the Pacific oyster. Assuming *AE* of 0.75 implies therefore that 45% of ingested N is excreted.

To highlight the differences between the modelling approaches with regard to predicted N_{ex}, the authors compared the methodology presented in this paper (model M1) to other modelling approaches. In model M2, the N_{ex} is a function of the oxygen utilisation rate and expressed as power functions of dry weight for starved and fed mussels (see Bayne and Scullard (1977) for equations; also Hawkins et al. (2002) and Brigolin et al. (2009) for similar applications to other bivalve species). Finally, in model M3, 45% of ingested N is excreted (Prins et al., 1995; Grangere et al., 2009). Comparison of the rates obtained for an individual mussel from the standalone DEB model forced with environmental conditions at site SN01 are presented in Figure 12. The model presented in this paper predicts a steady increase in N_{ex} through summer and autumn 2010 and a slight decrease in winter, followed by a substantial increase in spring 2011 along with increasing size of a mussel. M2 and M3 return highly variable excretion rates, and only M2 returns similar rates to M1 for a short period of time in December-January. Overall, M2 predicts a 27% lower rate and M3 a 45% higher when averaged annually. These differences will impact on primary productivity and thus on other components of the ecosystem, i.e. so called bottom-up control, with further implications for the accuracy of the ecological carrying capacity estimates.

It is worth noting that the inclusion of bivalve cultures in the model resulted in better representation of chlorophyll a concentrations (see Figure 10). However, as indicated before, the statistics for POC and PON are slightly worse and are generally poor for PON. This is largely due to the underestimation of late autumn and winter concentrations by the presented model. A possible reason is that increased storminess during this time of the year results in resuspension of sediments to the water column, including undecomposed detritus. However, in our model all detritus is instantaneously remineralised upon reaching the seabed. Inclusion of some form of a benthic model allowing for the exchange of fluxes of organic detritus through the water-sediment interface, such as that presented in Guyondet et al. (2010), may improve the model performance in this regard. Nevertheless, the presented model performs well during the productive season and is capable of predicting the annual pattern of blue mussel growth.

Chlorophyll a has been found as the best food proxy for determining the functional response of mussels (Eq.(3)) to food concentration and returning the best fit between the predicted and measured *L* and *DW*. POM, POC and PON and their combinations (e.g. POC/PON as a food quality determinant) have also been examined by the authors. Chlorophyll a has been commonly used as a food proxy in previous DEB model implementations (e.g. Filgueira et al., 2011; Rosland, 2009; Thomas et al., 2011; van der Veer, 2006; van der Meer, 2006). Ren et al. (2010)

point out after Dame and Prins (1998) that phytoplankton is the main source of food and energy to support large populations of bivalves in coastal systems; these authors could not reproduce the growth when POC was included as the food source. Handå et al. (2011) compared different food proxies and have not been able to identify a single best, as TPM, POM and chlorophyll a resulted in best fit at different locations. However, they recommended chlorophyll a as an overall good indicator of food availability for mussels. Similarly for oysters, Bourlès et al. (2009) concluded that the phytoplankton appears to be best food quantifier for forcing the DEB model of *C. gigas* and chlorophyll a was used in numerous other studies (e.g. Grangeré et al., 2009; Pouvreau et al., 2006). It is worth noting that although the functional response is determined by *Chla* in our model, we also allow for ingestion and assimilation of small detritus with the preference shifted towards the phytoplankton, i.e. μ_M in eqs. (4) and (5) equals 0.5 after Guyondet et al. (2010).

6 Conclusions

There is an increased interest in using computer models as tools to estimate ecological interactions and in estimation of the production and ecological carrying capacities in cultivated coastal regions. Mathematical models in use present different levels of complexity and recent attempts have been made towards dynamic modelling of feedbacks between shellfish cultures and the ecosystem.

The authors of this study developed a model describing the interactions between *Mytilus edulis* and the ecosystem, which forms a coupler between the DEB and NPZD models, and the coupled model was subsequently embedded within a numerical ocean model. The modelling system was applied to Bantry Bay in the south-west of Ireland, and successfully reproduced the biogeochemical cycles and growth of rope mussel cultures in the bay.

The presented model of the interactions between mussels and the ecosystem is consistent with the DEB model formulations and predicted changes in shellfish bio-energetics. It conserves mass by accounting for the allocation of relevant amounts of *C* and *N* in an organism, which brings this modelling attempt a step further from these recently reported. It is also recommended that for better representation of biodeposition by bivalve cultures and its effects on nutrient cycling these models are further expanded to describe benthic processes and their interactions with the pelagic environment.

This study adds to the growing evidence that models based on the DEB theory are capable of reproducing growth of various shellfish species in different environmental conditions. It also shows that impacts on ecosystem dynamics can be assessed using the presented modelling system making it a powerful tool to support sustainable management of shellfish aquaculture. The numerical models validated against observations remain an appropriate vehicle to further

our understanding of the complex interactions between ecological processes in coastal ecosystems.

Acknowledgements

This study is funded by the EU Interreg IVB Atlantic Area Programme and is part of the EASYCO (Collaborative European Atlantic Water Quality Forecasting System) project.

References

Alunno-Bruscia, M., Bourlès, Y., Maurer, D., Robert, S., Mazurié, J., Gangnery, A., Goulletquer, P., Pouvreau, S., 2011. A single bio-energetics growth and reproduction model for the oyster *Crassostrea gigas* in six Atlantic ecosystems. Journal of Sea Research 66(4), 340-348.

Barillé, L., Lerouxel, A., Dutertre, M., Haure, J., Barillé, A.-L., Pouvreau, S., Alunno-Bruscia, M., 2011. Growth of the Pacific oyster (*Crassostrea gigas*) in a high-turbidity environment: Comparison of model simulations based on scope for growth and dynamic energy budgets. Journal of Sea Research 66(4), 392-402.

Bayne, B.L., Scullard, C., 1977. Rates of nitrogen excretion by species of *Mytilus* (bivalvia: Mollusca). Journal of the Marine Biological Association of the United Kingdom 57, 355-369.

Bernard, I., de Kermoysan, G., Pouvreau, S., 2011. Effect of phytoplankton and temperature on the reproduction of the Pacific oyster *Crassostrea gigas*: Investigation through DEB theory. Journal of Sea Research 66(4), 349-360.

Bourlès, Y., Alunno-Bruscia, M., Pouvreau, S., Tollu, G., Leguay, D., Arnaud, C., Goulletquer, P., Kooijman, S.A.L.M., 2009. Modelling growth and reproduction of the Pacific oyster *Crassostrea gigas*: Advances in the oyster-DEB model through application to a coastal pond. Journal of Sea Research 62(2-3), 62-71.

Bricker, S.B., Ferreira, J.G., Simas, T., 2003. An integrated methodology for assessment of estuarine trophic status. Ecological Modelling 169, 39-60.

Brigolin, D., Dal Maschio, G., Rampazzo, F., Giani, M., Pastres, R., 2009. An individual-based population dynamic model for estimating biomass yield and nutrient fluxes through an off-

shore mussel (*Mytilus galloprovincialis*) farm. Estuarine, Coastal and Shelf Science 82, 365-376.

Browne, R., Deegan, B., Watson, L., MacGiolla Bhríde, D., Norman, M., Ó'Cinnéide, M., Jackson, D., O'Carroll, T., 2008. Status of Irish Aquaculture 2007. Report by Marine Institute, Bor Iascaigh Mhara and Údarás na Gaeltachta. December 2008, 142pp.

Cugier, P., Struski, C., Blanchard, M., Mazurié, J., Pouvreau, S., Olivier, F., Trigui, J.R., Thiébaut, E., 2010. Assessing the role of benthic filter feeders on phytoplankton production in a shellfish farming site: Mont Saint Michel Bay, France. Journal of Marine Systems 82, 21-34.

Dame, R.F., Prins, T.C., 1998. Bivalve carrying capacity in coastal ecosystems. Aquatic Ecology 31, 409-421.

Duarte, P., Meneses, R., Hawkins, A. J. S., Zhu, M., Fang, J., & Grant, J., 2003. Mathematical modelling to assess the carrying capacity for multi-species culture within coastal waters. Ecological Modelling 168(1-2), 109-143.

Duarte, P., Azevedo, B., Ribeiro, C., Pereira, A., Falcão, M., Serpa, D., Bandeira, R. and Reia J., 2007. Management oriented mathematical modelling of Ria Formosa (South Portugal). Transitional Waters Monographs 1, 13-51.

EC, 2000. Directive 2000/60/EC of the European Parliament and of the Council of 23 October 2000 establishing a framework for Community action in the field of water policy (EU Water Framework Directive). OJ L 327, 22.12.2000, 1–73.

EC, 2008. Directive 2008/56/EC of the European Parliament and of the Council of 17 June 2008 establishing a framework for Community action in the field of marine environmental policy (Marine Strategy Framework Directive). OJ L 164, 25.6.2008, 19–40.

Edwards, A., Jones, K., Graham, J.M., Griffiths, C.R., MacDougall, N., Patching, J., Richard, J.M., Raine, R., 1996. Transient coastal upwelling and water circulation in Bantry Bay, a ria on the SW coast of Ireland. Estuarine, Coastal and Shelf Science, 42, 213-230.

Egbert, G.D., Erofeeva, S.Y., 2002. Efficient inverse modeling of barotropic ocean tides. Journal of Atmospheric and Oceanic Technology 19(2), 183-204.

Emmery, A., Lefebvre, S., Alunno-Bruscia, M., Kooijmanm S.A.L.M., 2011. Understanding the dynamics of $\delta^{13}C$ and $\delta^{15}N$ in soft tissues of the bivalve *Crassostrea gigas* facing environmental fluctuations in the context of Dynamic Energy Budgets (DEB). Journal of Sea Research 66(4), 361-371.

Fairall, C.W., Bradley, E.F., Rogers, D.P., Edson, J.B., Young, G.S., 1996. Bulk parameterization of air–sea fluxes for tropical ocean-global atmosphere Coupled-Ocean Atmosphere Response Experiment. Journal of Geophysical Research 101, 3747–3764.

FAO, 2010. The State of World Fisheries and Aquaculture 2010. Rome, FAO. 2010. 197pp.

Fasham, M.J.R., Ducklow, H.W., McKelvie, S.M., 1990. A nitrogen-based model of plankton dynamics in the oceanic mixed layer. Journal of Marine Research 48, 591-639.

Fennel, K., Wilkin, J., Levin, L., Moisan, J., O'Reilly, J., Haidvogel, D., 2006. Nitrogen cycling in the Middle Atlantic Bight: Results from a three-dimensional model and implications for the North Atlantic nitrogen budget. Global Biogeochemical Cycles 20: GB3007 doi:10.1029/2005GB002456.

Ferreira, J.G., Hawkins, A.J.S., Bricker, S.B., 2007. Management of productivity, environmental effects and profitability of shellfish aquaculture - the Farm Aquaculture Resource Management (FARM) model. Aquaculture 264, 160-174. doi:10.1016/j.aquaculture.2006.12.017.

Ferreira, J.G., Hawkins, A.J.S., Monteiro, P., Moore, H., Service, M., Pascoe, P.L., Ramos, L., Sequeira, A., 2008. Integrated assessment of ecosystem-scale carrying capacity in shellfish growing areas. Aquaculture 275, 138-151. doi:10.1016/j.aquaculture.2007.12.018.

Filgueira, R., Grant, J., 2009. A box model for ecosystem-level management of mussel culture carrying capacity in a coastal Bay. Ecosystems 12, 1222-1233.

Filgueira, R., Rosland, R., Grant, J., 2011. A comparison of scope for growth (SFG) and dynamic energy budget (DEB) models applied to the blue mussel (*Mytilus edulis*). Journal of Sea Research 66(4), 403-410.

Garforth, D.B., FitzGerald, R., 1996. Opportunities in the Aquaculture Industry in the South West of Ireland. Report commisioned by South Western Services Ltd. And West Cork Leader Co-operative Society Ltd., 124pp.

Geider, R.J., MacIntyre, H.L., Kana, T.M., 1997. Dynamic model of phytoplankton growth and acclimation: responses of the balanced growth rate and the chlorophyll *a*:carbon ratio to light, nutrient-limitation and temperature. Marine Ecology Progress Series 148, 187-200.

Geider, R.J., MacIntyre, H.L., Kana, T.M., 1998. A dynamic regulatory model of phytoplanktonic acclimation to light, nutrients, and temperature. Limnology and Oceanography 43(4), 679-694.

Gnaiger, E., Forstner, H., 1983. Polarographic Oxygen Sensors: Aquatic and Physiological Applications. Berlin, Springer. XII, 370pp.

Grangeré, K., Ménesguen, A., Lefebvre, S., Bacher, C., Pouvreau, S., 2009. Modelling the influence of environmental factors on the physiological status of the Pacific oyster *Crassostrea gigas* in an estuarine embayment; The Baie des Veys (France). Journal of Sea Research 62(2-3), 147-158.

Grangeré, K., Lefebvre, S., Bacher, C., Cugier, P., Ménesguen, A., 2010. Modelling the spatial heterogeneity of ecological processes in an intertidal estuarine bay: dynamic interactions between bivalves and phytoplankton. Marine Ecology Progress Series 415, 141-158.

Grant, J., Bacher, C., Cranford, P.J., Guyondet, T., Carreau, M., 2008. A spatially explicit ecosystem model of seston depletion in dense mussel culture. Journal of Marine Systems 73, 155-168.

Guyondet, T., Roy, S., Koutitonsky, V.G., Grant, J., Guglielmo, T., 2010. Integrating multiple spatial scales in the carrying capacity assessment of a coastal ecosystem for bivalve aquaculture. Journal of Sea Research 64, 341-359.

Handå, A., Alver, M., Edvardsen, C.V., Halstensen, S., Olsen, A.J., Øie, G., Reitan, K.I., Olsen, Y., Reinertsen, H., 2011. Growth of farmed blue mussel (*Mytilus edulis* L.) in a Norwegian coastal area; comparison of food proxies by DEB modeling. Journal of Sea Research, 66(4), 297-307.

Hawkins, A.J.S., Duarte, P., Fang, J.G., Pascoe, P.L., Zhang, J.H., Shang, X.L., Zhu, M.Y., 2002. A functional model of responsive suspension-feeding and growth in bivalve shellfish,

configured and validated for the scallop *Chlamys farreri* during culture in China. Journal of Experimental Marine Biology and Ecology 281, 13-40.

Kooijman, S.A.L.M., 2010. Dynamic Energy Budget Theory for Metabolic Organisation, 3rd edition. Cambridge University Press, Cambridge, 2010. 514pp.

Krishnakumar, P.K., Casillas, E., Varanasi, U., 1994. Effect of environmental contaminants on the health of *Mytilus edulis* from Puget Sound, Washington, USA. I. Cytochemical measures of lysosomal responses in the digestive cells using automatic image analysis. Marine Ecology Progress Series 106, 249-261.

Maar, M., Bolding, K., Petersen, J.K., Hansen, J.L.S., Timmermann, K., 2009. Local effects of blue mussels around turbine foundations in an ecosystem model of Nysted off-shore wind farm, Denmark. Journal of Sea Research 62(2-3), 159-174.

Marinov, D., Galbiati, L., Giordani, G., Viaroli, P., Norro, A., Bencivelli, S., Zaldívar, J.-M., 2007. An integrated modelling approach for the management of clam farming in coastal lagoons. Aquaculture 269, 306-320.

Newell, C.R., Campbell, D.E., Gallagher, S.M., 1998. Development of the mussel aquaculture lease site model MUSMOD©: a field program to calibrate model formulations. Journal of Experimental Marine Biology and Ecology 219, 143-169.

Nunes, J.P., Ferreira, J.G., Bricker, S.B., O'Loan, B., Dabrowski, T., Dallaghan, B., Hawkins, A., O'Connor, B., O'Carroll, T., 2011. Towards an ecosystem approach to aquaculture: Assessment of sustainable shellfish cultivation at different scales of space, time and complexity. Aquaculture 315, 369-383. doi:10.1016/j.aquaculture.2011.02.048.

Piman, T., Babel, M.S., Das Gupta, A., Weesakul, S., 2007. Development of a window correlation matching method for improved radar rainfall estimation. Hydrology and Earth System Sciences 11, 1361-1372.

Platt, T., Irwin, B., 1973. Caloric content of phytoplankton. Limnology and Oceanography 18, 306-310.

Pouvreau, S., Bourlès, Y., Lefebvre, S., Gangnery, A., Alunno-Bruscia, M., 2006. Application of a dynamic energy budget model to the Pacific oyster, *Crassostrea gigas*, reared under various environmental conditions. Journal of Sea Research 56, 156-167.

Prins, T.C., Escaravage, V., Smaal, A.C., Peeters, J.C.H., 1995. Nutrient cycling and phytoplankton dynamics in relation to mussel grazing in a mesocosm experiment. Ophelia 41, 289-315.

Raine, R., McMahon, T., O'Mahoney, J., Moloney, M. and Roden, C. 1990. Water circulation and phytoplankton populations in two estuaries on the west coast of Ireland, in: Chambers, P. L., Chambers, C. M. (Eds.), Estuarine Ecotoxicology. JAPAGA, Wicklow, Ireland, pp. 19-28.

Raine, R., Joyce, B., Richard, J., Pazos, Y., Moloney, M., Jones, K., Patching, J.W., 1993. The development of an exceptional bloom of the dinoflagellate *Gyrodinium aureolum* on the southwest Irish coast. ICES Journal of Marine Science 50, 461-469.

Ren, J.S., Ross, A.H., Hadfield, M.G., Hayden, B.J., 2010. An ecosystem model for estimating potential shellfish culture production in sheltered coastal waters. Ecological Modelling 221, 527-539.

Rodhouse, P.G., Roden, C.M., Hensey, M.P., Ryan, T.H., 1984. Resource allocation in *Mytilus edulis* on the shore and in suspended culture. Marine Biology 84, 27-34.

Rosland, R., Strand, Ø., Alunno-Bruscia, M., Bacher, C., Strohmeier, T., 2009. Applying Dynamic Energy Budget (DEB) theory to simulate growth and bio-energetics of blue mussels under low seston conditions. Journal of Sea Research 62(2-3), 49-61.

Rosland, R., Bacher, C., Strand, Ø., Aure, J., Strohmeier, T., 2011. Modelling growth variability in longline mussel farms as a function of stocking density and farm design. Journal of Sea Research 66(4), 318-330.

Saraiva, S., van der Meer, J., Kooijman, S.A.L.M., Sousa, T., 2011a. DEB parameters estimation for *Mytilus edulis*. Journal of Sea Research 66(4), 289-296.

Saraiva, S., van der Meer, J., Kooijman, S. A. L. M., Sousa, T., 2011b. Modelling feeding processes in bivalves: A mechanistic approach. Ecological Modelling 222(3), 514-523.

Shchepetkin, A.F., McWilliams, J.C., 2005. The regional oceanic modeling (ROMS): a split-explicit, free-surface, topography-following-coordinate oceanic model. Ocean Modelling 9, 347-404.

Taylor, K.E., 2001. Summarizing multiple aspects of model performance in a single diagram. Journal of Geophysical Research 106, 7183-7192.

Thomas, Y., Mazurié, J., Alunno-Bruscia, M., Bacher, C., Bouget, J.-F., Gohin, F., Pouvreau, S., Struski, C., 2011. Modelling spatio-temporal variability of Mytilus edulis (L.) growth by forcing a dynamic energy budget model with satellite-derived environmental data. Journal of Sea Research 66(4), 308-317.

van der Meer, J., 2006. An introduction to Dynamic Energy Budget (DEB) models with special emphasis on parameter estimation. Journal of Sea Research 56, 85-102.

van der Veer, H.W., Cardoso, J.F.M.F., van der Meer, J., 2006. The estimation of DEB parameters for various Northeast Atlantic bivalve species. Journal of Sea Research 56, 107-124.

van Haren, R.J.F., Kooijman, S.A.L.M., 1993. Application of a dynamic energy budget model to *Mytilus edulis* (L.). Netherlands Journal of Sea Research 31(2), 119-133.

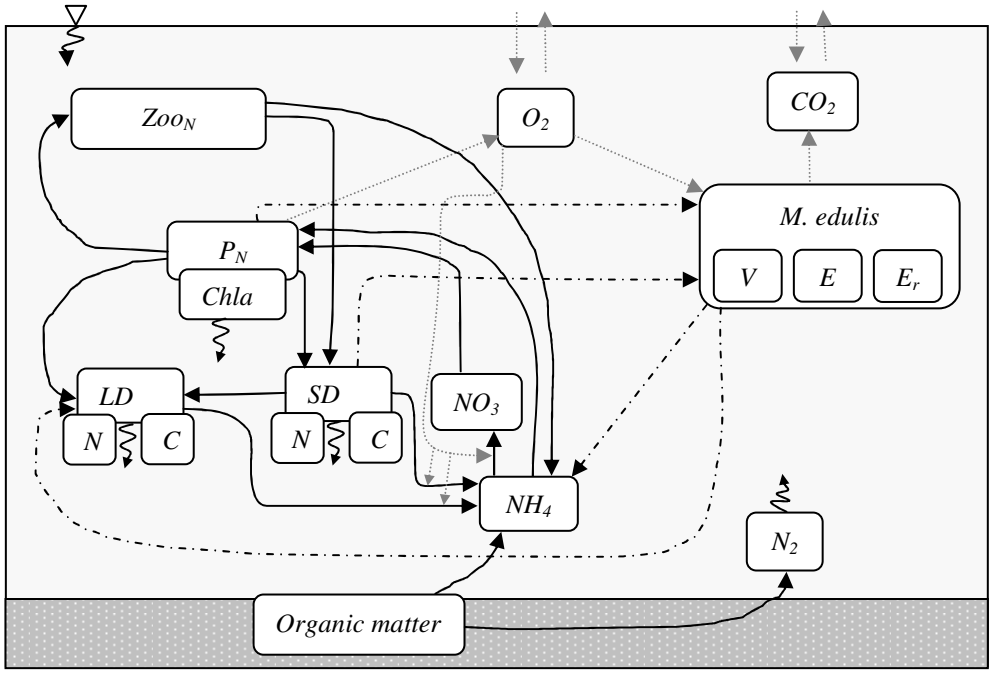

Figure 1. A schematic diagram of coupled DEB-NPZD model. Model state variables are: Zoo_N – zooplankton (mmol N m^{-3}), P_N – phytoplankton (mmol N m^{-3}), *Chla* – chlorophyll a (mg m^{-3}), LD_N and SD_N – large and small detritus nitrogen, respectively (mmol N m^{-3}), LD_C and SD_C – large and small detritus carbon, respectively (mmol C m^{-3}), NO_3 – nitrate (mmol N m^{-3}), NH_4 – ammonium (mmol N m^{-3}), O_2 – oxygen (mmol O_2 m^{-3}), V – volume of a bivalve (m^3), E – energy reserves of a bivalve (J) and E_r – reproductive energy of a bivalve (J).

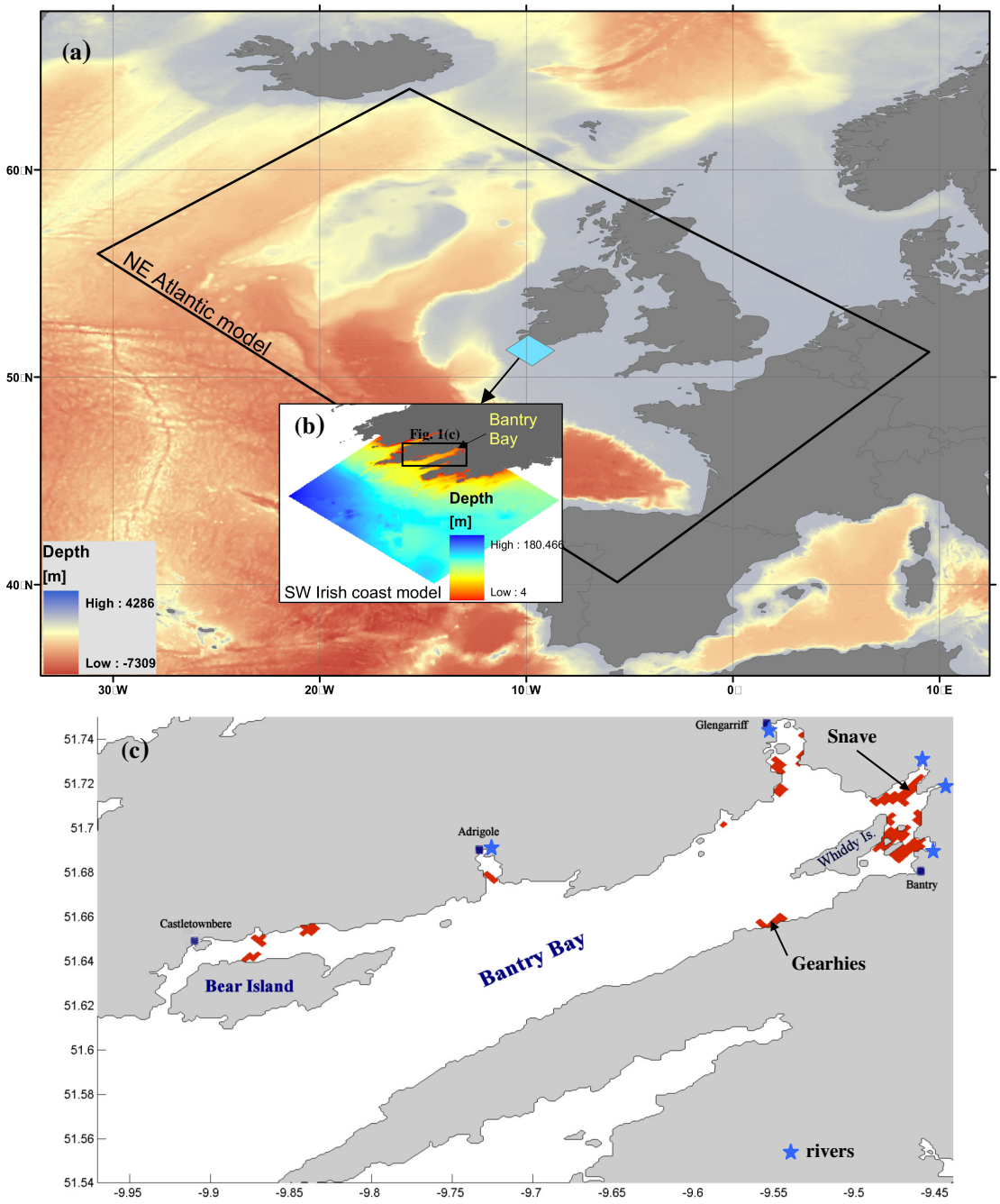

Figure 2. Maps showing the (a) bathymetry and extents of the NE Atlantic 'parent' model, (b) bathymetry and extents of the nested model of SW Irish coast and (c) distribution of rope mussel farms (red polygons) in Bantry Bay and locations of Snave and Gearhies sampling stations.

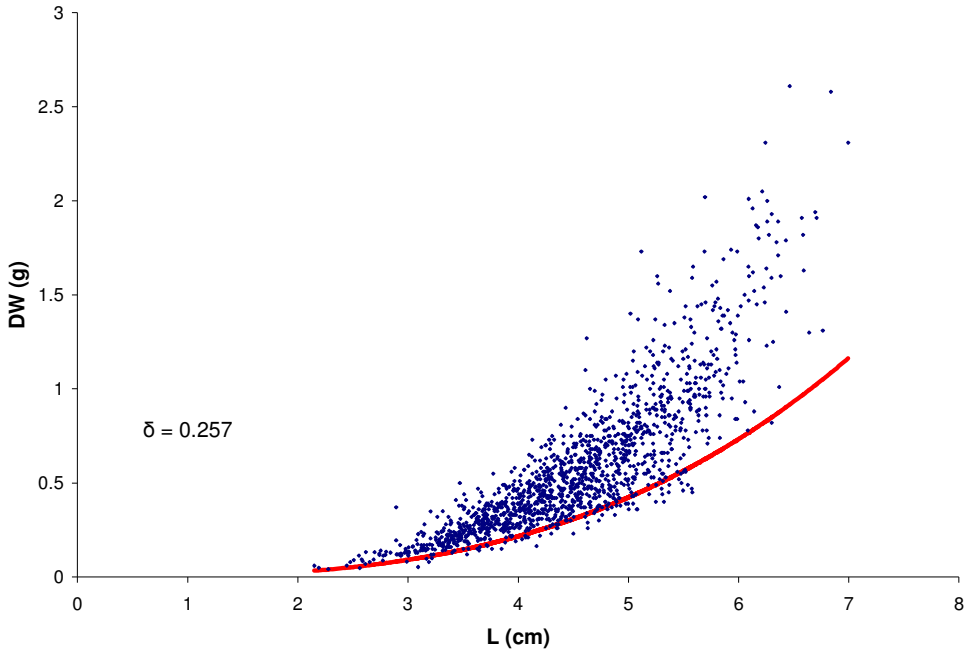

Figure 3. Shell length plotted against dry weights for pooled data from four sites in Bantry Bay. The line shows the relationship between the structural volume and shell length for the shape coefficient of 0.257, which was obtained following the methodology described in section 4.1.

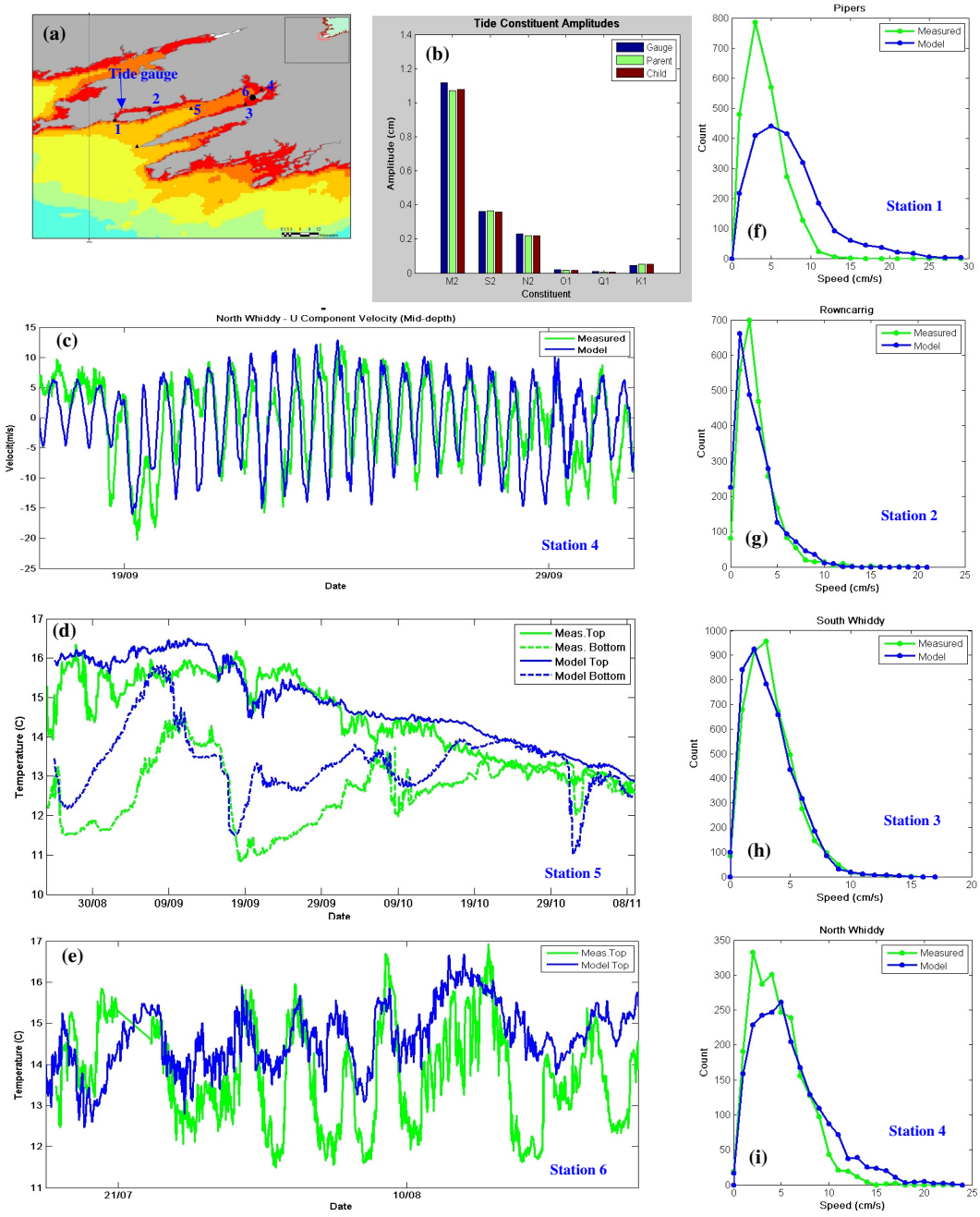

Figure 4. Validation of the hydrodynamic model: (a) stations locations and numbering, (b) tidal constituents at Castletownbere tide gauge, (c) time series of mid-depth U-component of current velocity at station 4 (North Whiddy), (d) time series of surface (top) and bottom water temperatures at station 5, (e) time series of surface water temperatures at station 6, (f-i) depth-integrated current speeds histograms.

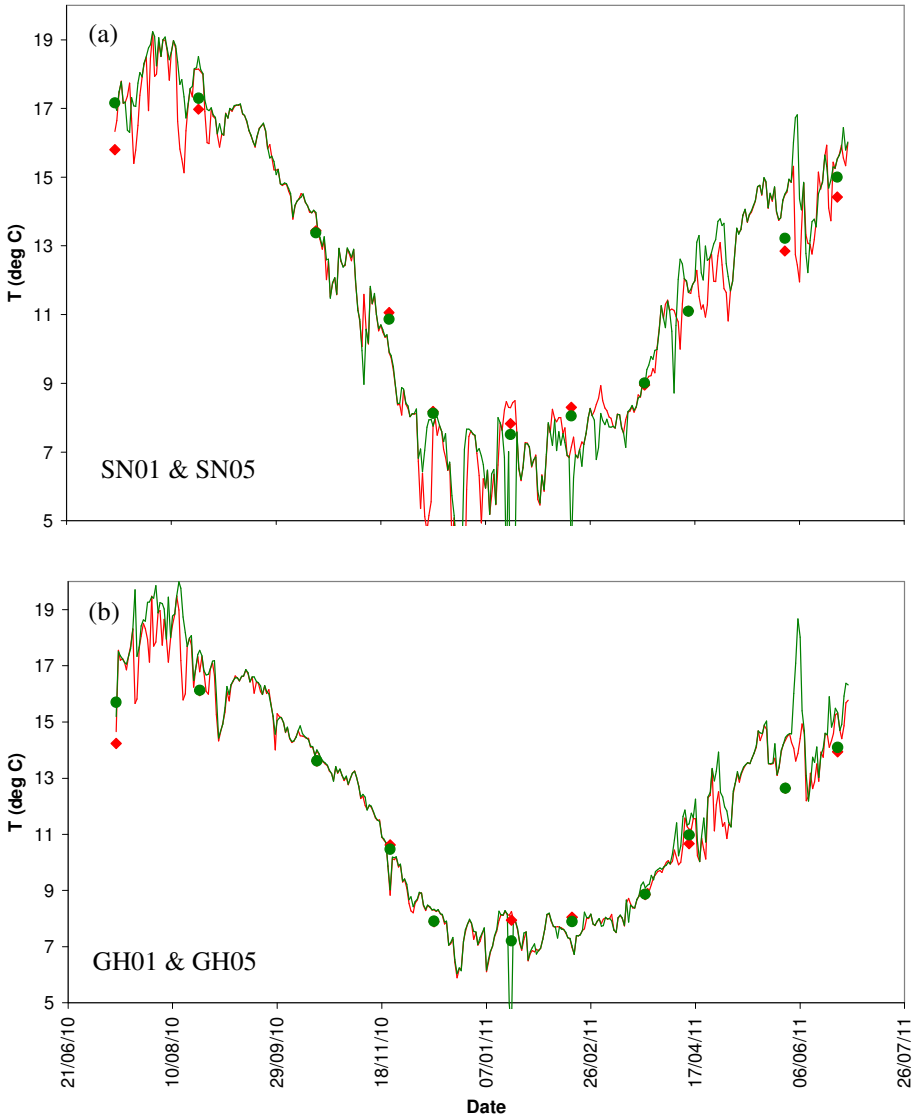

Figure 5. Comparison of measured and model predicted water temperatures at (a) Snave and (b) Gearhies sites; green – 1m depth, red – 5m depth.

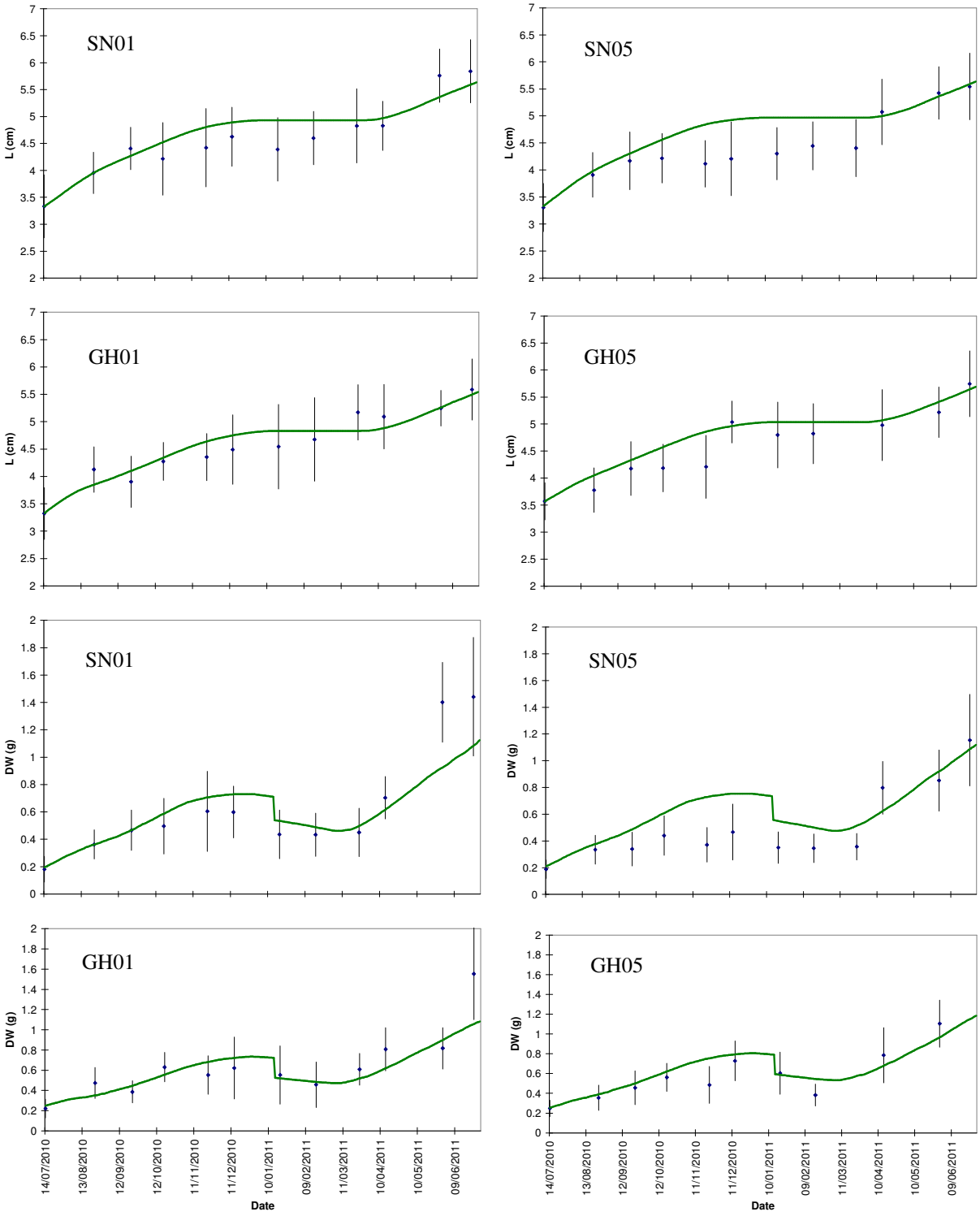

Figure 6. Observed (dots with bars for standard deviation) and simulated shell lengths and dry weights of *M.edulis* predicted by the numerical model for four sites in Bantry Bay: Snave 1m depth (SN01), Snave 5m depth (SN05), Gearhies 1m depth (GH01) and Gearhies 5m depth (GH05).

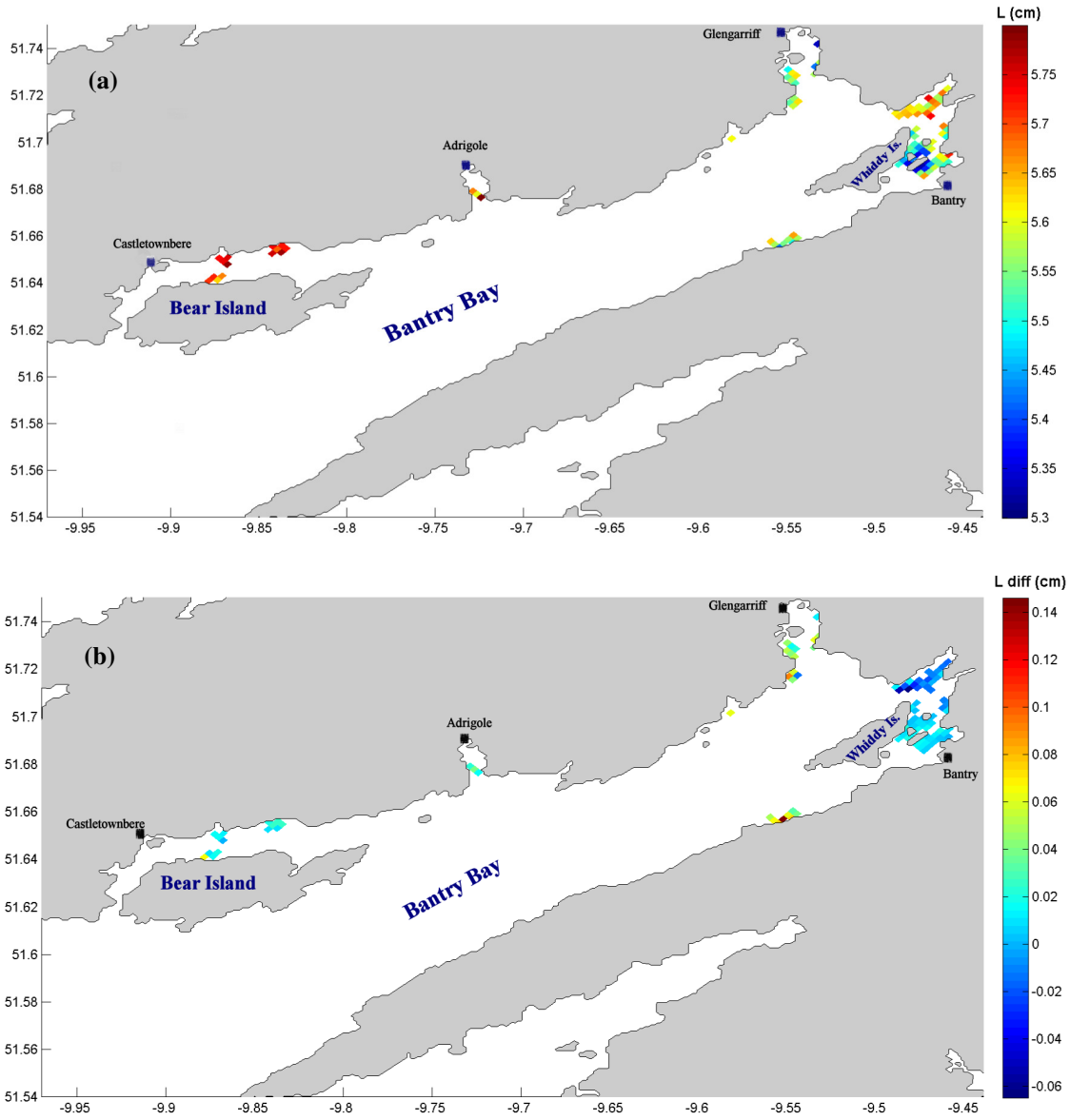

Figure 7. Predicted shell length at the end of the simulation on 29th June 2011 (a) and difference in the predicted shell length between the bottommost and topmost ends of dropper lines on the same date (b).

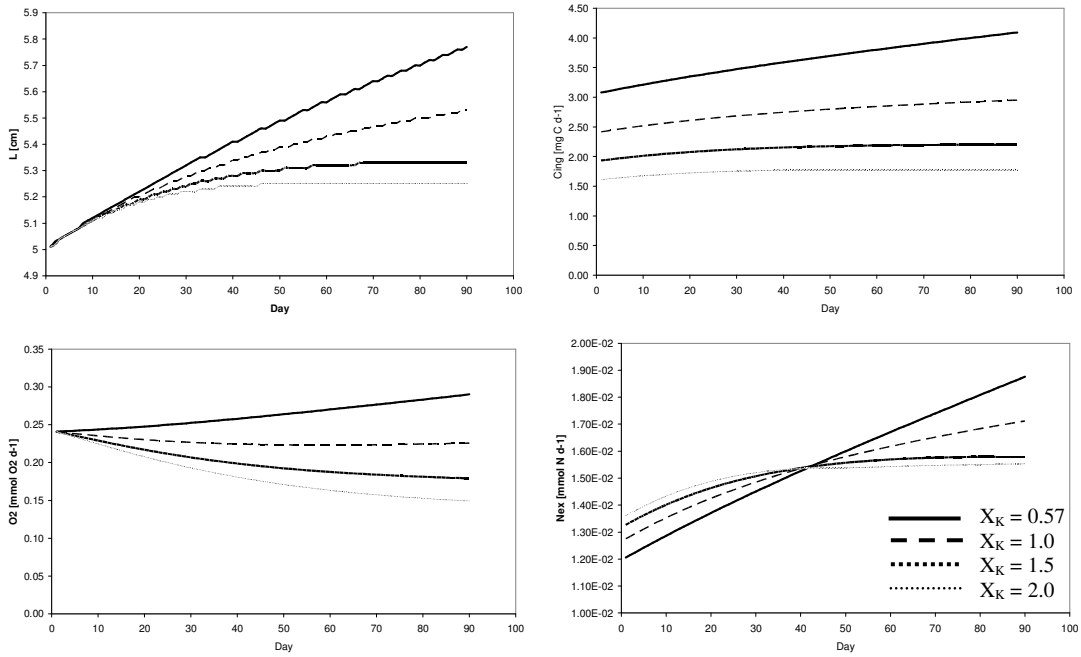

Figure 8. Results of a sensitivity study of a standalone DEB-NPZD model in idealized conditions.

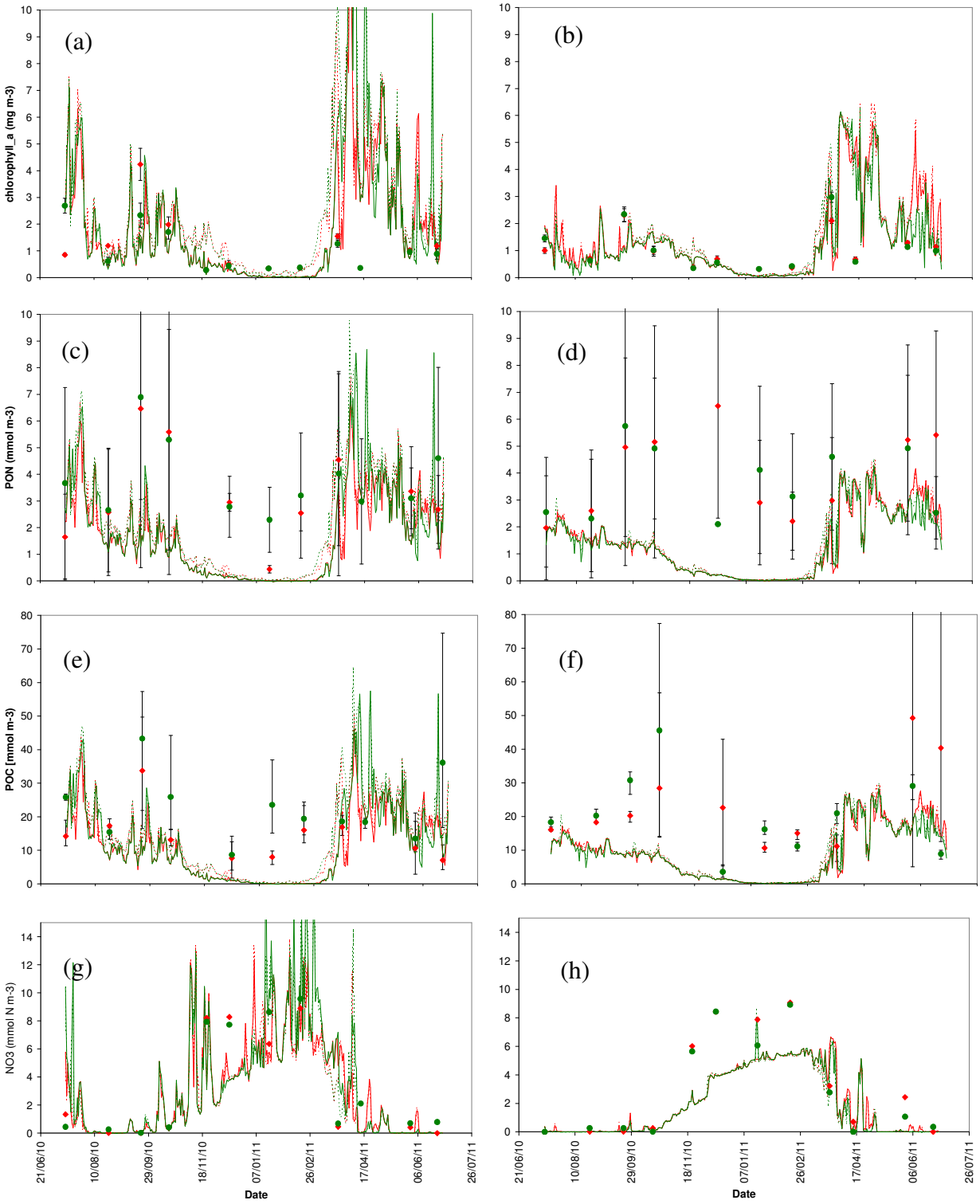

Figure 9. Comparison of measured and model predicted chlorophyll a, particulate organic nitrogen, particulate organic carbon and nitrate concentrations at Snave (left column) and Gearhies (right column) sites; green – 1m depth, red – 5m depth; solid lines – coupled DEB-NPZD model; broken lines – no mussels.

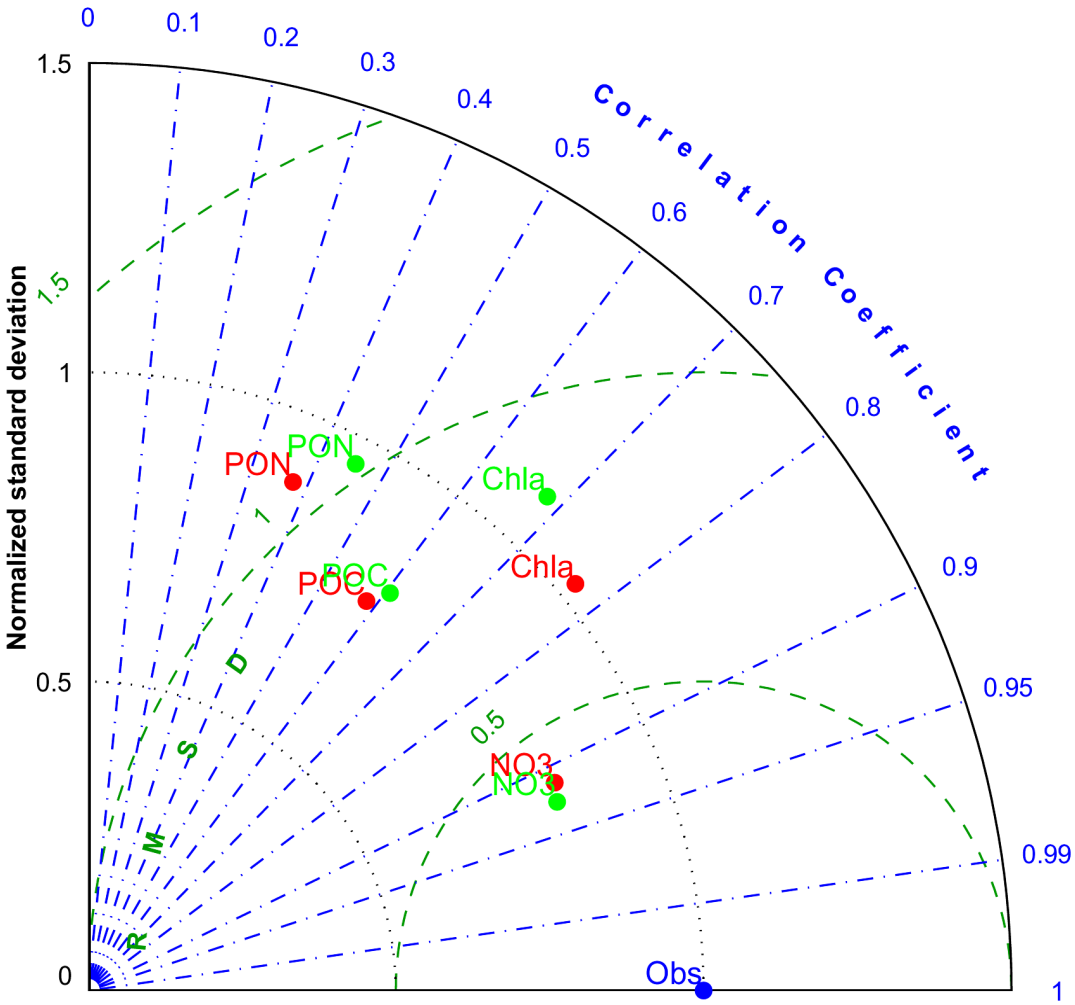

Figure 10. Taylor diagram comparing the model predictions and observations of chlorophyll a, particulate organic carbon, particulate organic nitrogen and nitrate concentrations at four sites in Bantry Bay: SN01, SN05, GH01 and GH05; red – model with mussels, green – model without mussels.

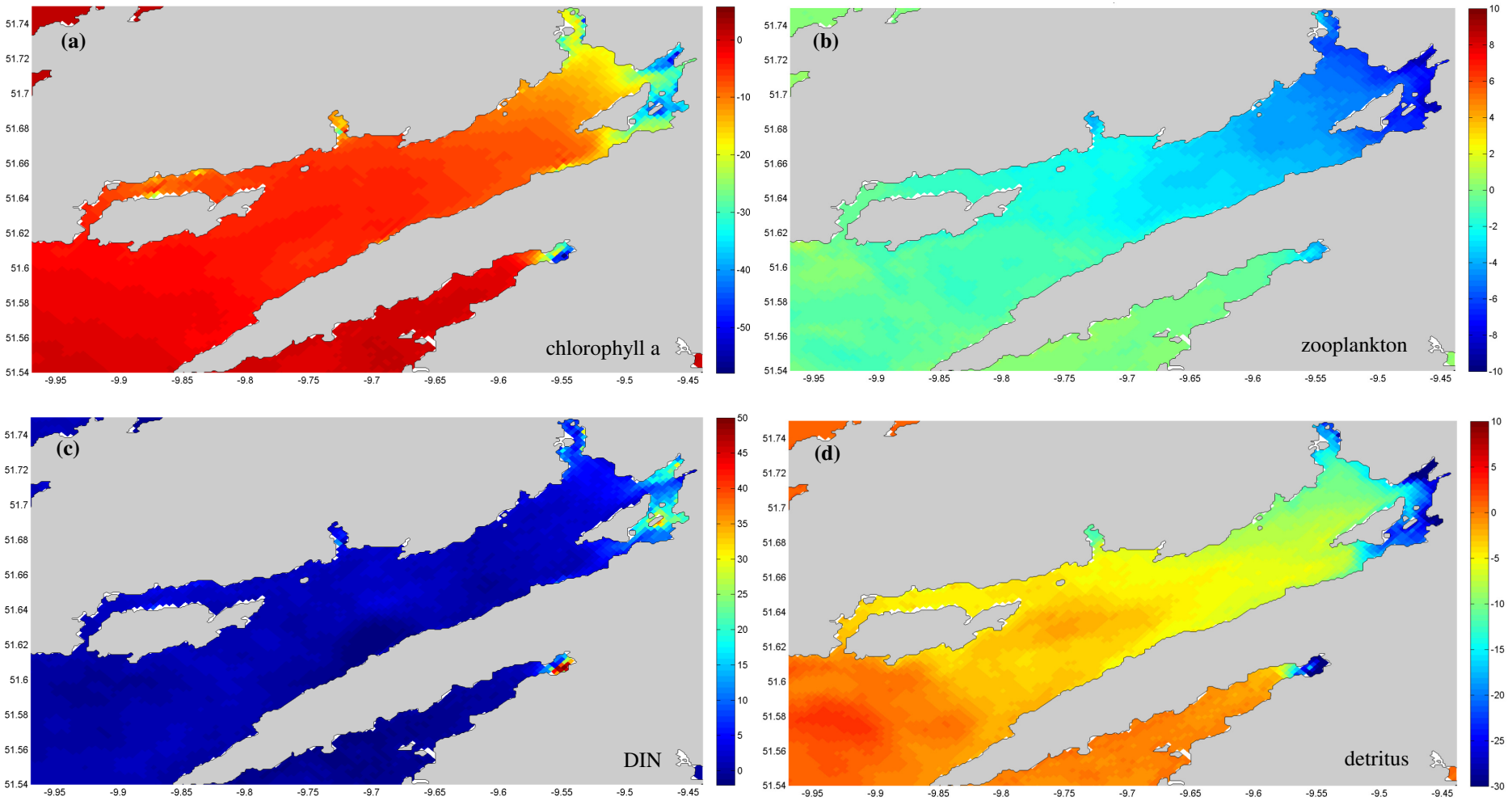

Figure 11. Predicted impacts of cultured mussels on the concentration of chlorophyll_a (a), zooplankton (b), DIN (c) and detritus (d) shown as the percentage change from the scenario without mussels and averaged over the simulation period, 14 July 2010 – 29 June 2011.

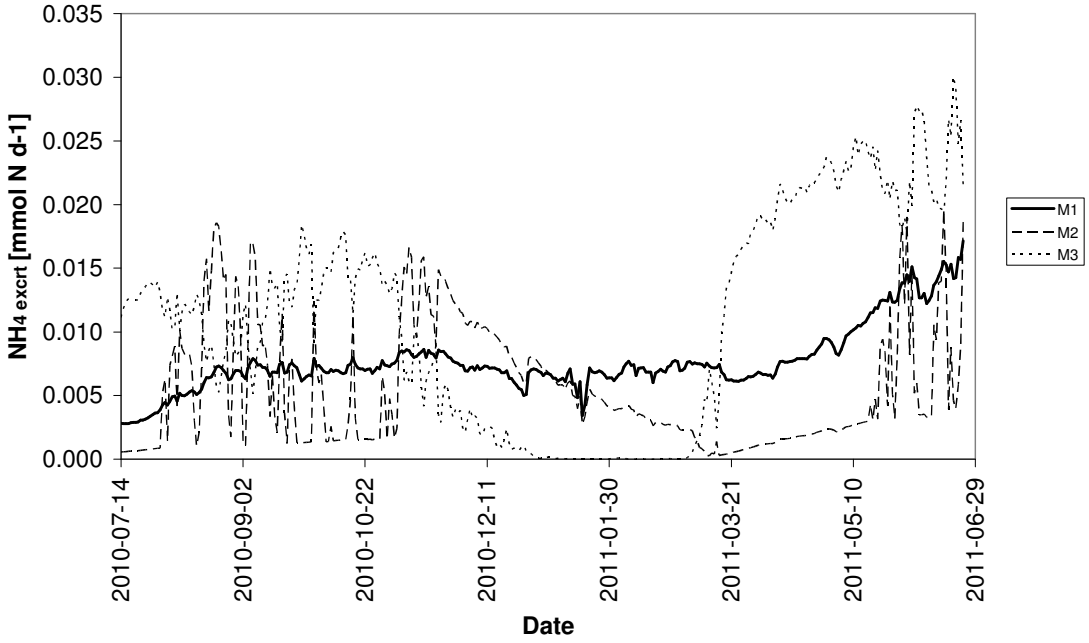

Figure 12. Comparison of the ammonium excretion rates by an individual mussel at site SN01 predicted by the model developed by the authors (M1), the model relating the excretion rate to the oxygen consumption rate (M2) and the rate expressed as a fixed fraction of N ingested (M3).

Table 1. Summary of the DEB model formulations.

Parameter	Equation	Unit
Energy ingestion rate	$\dot{p}_X = \{\dot{p}_{Xm}\}\frac{X}{X+X_K}V^{2/3}$	J d^{-1}
Energy assimilation rate	$\dot{p}_A = AE\cdot\dot{p}_X$	J d^{-1}
Energy utilization rate	$\dot{p}_C = \frac{[E]}{[E_G]+\kappa\cdot[E]}\left(\frac{[E_G]\{\dot{p}_{Am}\}V^{2/3}}{[E_m]}+[\dot{p}_M]V\right)$	J d^{-1}
Maturity maintenance	$\dot{p}_J = \left(\frac{1-\kappa}{\kappa}\right)Min(V,V_p)[\dot{p}_M]$	J d^{-1}
Rate of change of bivalve volume	$\frac{dV}{dt} = (\kappa\cdot\dot{p}_C - \dot{p}_M)/[E_G]$	cm^3 d^{-1}
Flow to energy reserves	$\frac{dE}{dt} = \dot{p}_A - \dot{p}_C$	J d^{-1}
Flow to reproductive buffer	$\frac{dE_r}{dt} = (1-\kappa)\dot{p}_C - \dot{p}_J$	J d^{-1}
Temperature correction factor (for $\{\dot{p}_{Xm}\}$ and $[\dot{p}_M]$)	$T_{corr} = \frac{e^{\left(\frac{T_A}{T_{ref}}-\frac{T_A}{T}\right)}}{1+e^{\left(\frac{T_{AL}}{T}-\frac{T_{AL}}{T_L}\right)}+e^{\left(\frac{T_{AH}}{T_H}-\frac{T_{AH}}{T}\right)}}$	-
Symbols:		
$\{\dot{p}_{Xm}\}$ - maximum ingestion rate		J cm^{-2} d^{-1}
X – food density		mg m^{-3}
X_K – saturation coefficient for food		mg m^{-3}
V – structural body volume		cm^{-3}
AE – assimilation efficiency		-
$[E]$ – energy density		J cm^{-3}
$[E_G]$ – volume-specific costs for structure		J cm^{-3}
$\{\dot{p}_{Am}\}$ - maximum surface-area-specific assimilation rate		J cm^{-2} d^{-1}
$[E_m]$ – maximum energy density of the reserves		J cm^{-3}
κ – fraction of energy spent on maintenance and growth		-
$[\dot{p}_M]$ - volume-specific maintenance costs		J cm^{-2} d^{-1}
V_p – volume at maturity		cm^3
T – absolute water temperature		K
T_{AL} – rate of decrease at lower boundary		K
T_{AH} – rate of decrease at upper boundary		K
T_L – lower boundary of tolerance range		K

T_H – upper boundary of tolerance range		K
T_A – Arrhenius temperature		K
T_{ref} – reference temperature		K

Table 2. Parameterization of the DEB-NPZD model.

Parameter	Symbol	Unit	Value	Source
DEB model parameters:[l]				
Volume-specific maintenance costs	$\dot{p}_M$	J cm^{-3} d^{-1}	32.3 (11.6[a]-32.3[b])	This study
Fraction of utilized energy spent on maintenance and growth	κ	-	0.72 (0.45[b]-0.8[d])	This study
Half-saturation coefficient for chlorophyll a	X_k	mg m^{-3}	0.57 (0.41-3.30)[e]	This study
Shape coefficient	δ	-	0.257 (0.231[b]-0.333[f])	This study
DEB-NPZD coupler parameters:				
Conversion factor from WW to DW	Ψ_{DW_WW}	-	0.2	b, g
Conversion factor from WW to AFDW	Ψ_{DW_AFDW}	-	0.12	c
Specific density of *M. edulis*	ρ	g cm^{-3}	1.0	h
Energy content of the reserves in AFDW	μ_E	J g^{-1}	23,000	c
Constant for converting oxygen to energy equivalents	η	J mg^{-1} O_2	14.3	b, i
Phytoplankton C:N ratio	P_{CN}	mol C mol^{-1} N	6.625	j
Food selection factor	μ_M	-	0.5	k
Energetic value of the phytoplankton C	P_{EC}	cal mg^{-1} C	11.4	l
Conversion factor from calories to Joules	c_f	J cal^{-1}	4.189	b
Assimilation efficiency of food	AE	-	0.75	c
C fraction of AFDW	$AFDW_C$	-	0.4	c
M. edulis C:N ratio in flesh	M_{CN}	mol C mol^{-1} N	4.82	m
Fraction of C allocated in flesh	Ψ_{C_flesh}	-	0.92	m
Fraction of N allocated in flesh	Ψ_{N_flesh}	-	0.88	m
Fraction of C allocated in shell	Ψ_{C_shell}	-	0.08	m
Fraction of N allocated in shell	Ψ_{N_shell}	-	0.12	m

[l] Parameters not listed are as in van der Veer et al. (2006)
[a] Saraiva et al. (2011)
[b] Rosland et al. (2009)
[c] van der Veer et al. (2006)
[d] http://www.bio.vu.nl/thb/research/index.html (last accessed 30 April 2012)
[e] Filgueira et al. (2011)
[f] van der Meer (2006)
[g] Krishnakumar et al. (1994)
[h] van Haren and Kooijman (1993)
[i] Gnaiger and Forstner (1983)
[j] Fasham et al. (1990)
[k] Guyondet et al. (2010)
[l] Platt and Irwin (1973)
[m] Rodhouse et al. (1984)